Progress in membrane distillation processes for dye wastewater treatment: A review

Lebea N. Nthunya, Kok Chung Chong, Soon Onn Lai, Woei Jye Lau, Eduardo Alberto López-Maldonado, Lucy Mar Camacho, Mohammad Mahdi A. Shirazi, Aamer Ali, Bhekie B. Mamba, Magdalena Osial, Paulina Pietrzyk-Thel, Agnieszka Pregowska, Oranso T. Mahlangu

PII: S0045-6535(24)01240-2

DOI: https://doi.org/10.1016/j.chemosphere.2024.142347

Reference: CHEM 142347

To appear in: *ECSN*

Received Date: 11 March 2024

Revised Date: 26 April 2024

Accepted Date: 14 May 2024

Please cite this article as: Nthunya, L.N., Chong, K.C., Lai, S.O., Lau, W.J., López-Maldonado, E.A., Camacho, L.M., Shirazi, M.M.A., Ali, A., Mamba, B.B., Osial, M., Pietrzyk-Thel, P., Pregowska, A., Mahlangu, O.T., Progress in membrane distillation processes for dye wastewater treatment: A review, *Chemosphere*, https://doi.org/10.1016/j.chemosphere.2024.142347.

Progress in membrane distillation processes for dye wastewater treatment: A review

Lebea N. Nthunya[1*], Kok Chung Chong[2,3], Soon Onn Lai[2,3], Woei Jye Lau[4], Eduardo Alberto López-Maldonado[5], Lucy Mar Camacho[6], Mohammad Mahdi A. Shirazi[7], Aamer Ali[7], Bhekie B. Mamba[8], Magdalena Osial[9], Paulina Pietrzyk-Thel[9], Agnieszka Pregowska[9], Oranso T. Mahlangu[8*]

[1] Molecular Sciences Institute, School of Chemistry, University of the Witwatersrand, Private Bag X3, 2050, Johannesburg, South Africa

[2] Department of Chemical Engineering, Lee Kong Chian Faculty of Engineering and Science, Universiti Tunku Abdul Rahman, Jalan Sungai Long, Kajang 43000, Selangor, Malaysia

[3] Centre of Photonics and Advanced Materials Research, Universiti Tunku Abdul Rahman, Kampar 31900, Perak, Malaysia

[4] Advanced Membrane Technology Research Centre (AMTEC), Faculty of Chemical and Energy Engineering, Universiti Teknologi Malaysia, Johor Bahru 81310, Johor, Malaysia

[5] Faculty of Chemical Sciences and Engineering, Autonomous University of Baja, California, CP, Tijuana 22390, Baja California, Mexico

[6] Department of Environmental Engineering, Texas A&M University-Kingsville, MSC 2013, 700 University Blvd., Kingsville, TX 78363, USA

[7] Centre for Membrane Technology, Department of Chemistry and Bioscience, Aalborg University, Fredrik Bajers Vej 7H, 9220 Aalborg, Denmark

[8] Institute for Nanotechnology and Water Sustainability, College of Science, Engineering and Technology, University of South Africa, Florida Science Campus, 1709 Roodepoort, South Africa

[9] Institute of Fundamental Technological Research, Polish Academy of Sciences, Pawińskiego 5B, 02-106 Warszawa

*Corresponding author. E-mail address: nthunyalebea@gmail.com

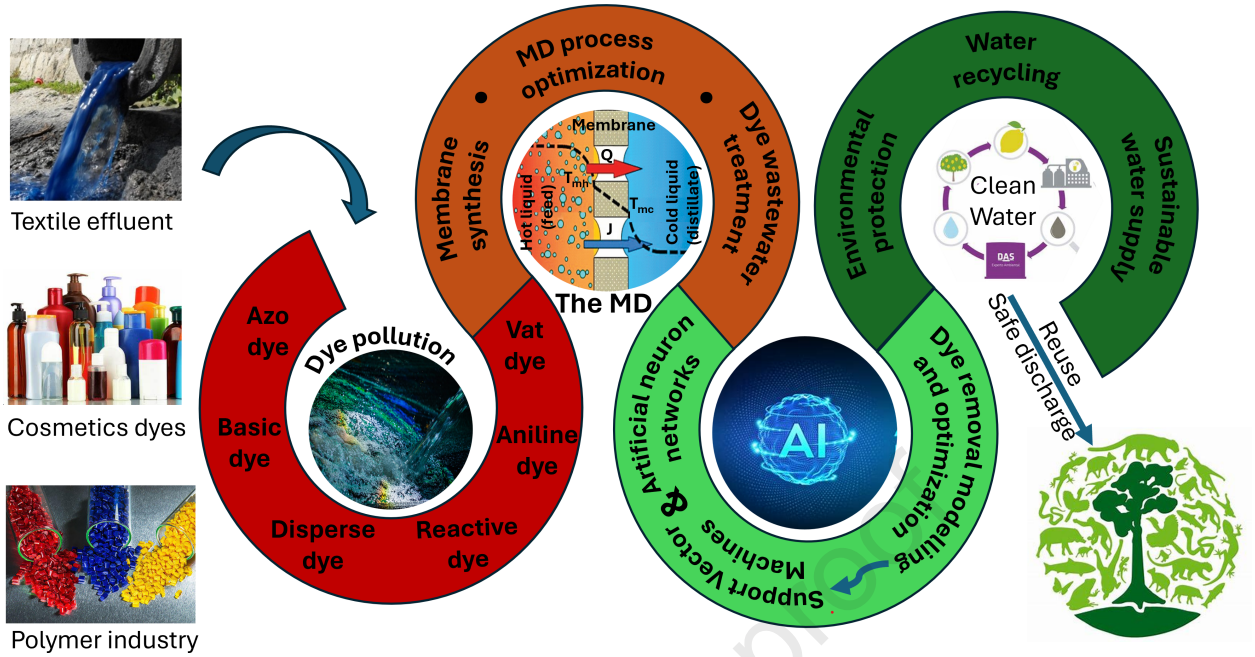

Progress in membrane distillation processes for dye wastewater treatment: A review

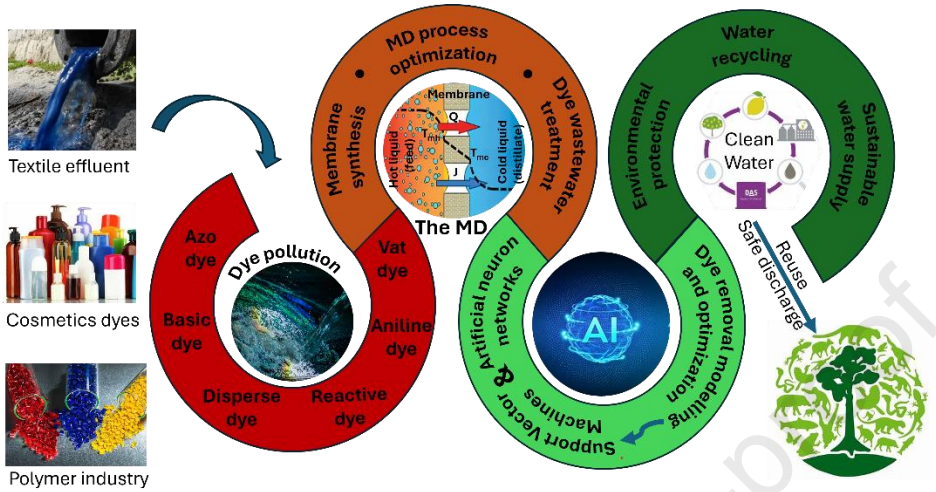

Graphical abstract

Abstract

Textile and cosmetic industries generate large amounts of dye effluents requiring treatment before discharge. This wastewater contains high levels of reactive dyes, low to none-biodegradable materials and chemical residues. Technically, dye wastewater is characterised by high chemical and biological oxygen demand. Biological, physical and pressure-driven membrane processes have been extensively used in textile wastewater treatment plants. However, these technologies are characterised by process complexity and are often costly. Also, process efficiency is not achieved in cost-effective biochemical and physical treatment processes. Membrane distillation (MD) emerged as a promising technology harnessing challenges faced by pressure-driven membrane processes. To ensure high cost-effectiveness, the MD can be operated by solar energy or low-grade waste heat. Herein, the MD purification of dye wastewater is

comprehensively and yet concisely discussed. This involved research advancement in MD processes towards removal of dyes from industrial effluents. Also, challenges faced by this process with a specific focus on fouling are reviewed. Current literature mainly tested MD setups in the laboratory scale suggesting a deep need of further optimization of membrane and module designs in near future, especially for textile wastewater treatment. There is a need to deliver customized high-porosity hydrophobic membrane design with the appropriate thickness and module configuration to reduce concentration and temperature polarization. Also, energy loss should be minimized while increasing dye rejection and permeate flux. Although laboratory experiments remain pivotal in optimizing the MD process for treating dye wastewater, their time-intensive nature poses a challenge. Given the multitude of parameters involved in MD process optimization, artificial intelligence (AI) methodologies present a promising avenue for assistance. Thus, AI-driven algorithms have the potential to enhance overall process efficiency, cutting down on time, fine-tuning parameters, and driving cost reductions. However, achieving an optimal balance between efficiency enhancements and financial outlays is a complex process. Finally, this paper suggests a research direction for the development of effective synthetic and natural dye removal from industrially discharged wastewater.

Keywords: Energy Consumption; Dye Effluent; Fouling; Heat and Mass Transfer; Membrane and Module Design; Membrane Distillation

List of Acronyms

ANNs	Artificial neuron networks	PEI	Polyetherimide

AGMD	Air gap membrane distillation	PES	polyether sulfone
AgNPs	Silver nanoparticles	pH_{pzc}	Point of zero charge
AI	Artificial Intelligence	PP	Polypropylene
CFD	Computational fluid dynamics	PS	Polystyrene
CI	Colour index	PTFE	Polytetrafluoroethylene
CNTs	Carbon nanotubes	PU	Polyurethane
CP	Concentration polarization	PVA	Poly(vinylalcohol)
CR	Congo red dye	PVDF	Polyvinylidene fluoride
DCMD	Direct contact membrane distillation	PVDF-HFP	Poly(vinylidene fluoride-co-hexafluoropropene)
HFP	Hexafluoropropylene	SAN	Styrene acrylonitrile
HIPS	High-impact polystyrene	SBMA	Sulfobetaine methacrylate
LEP	Liquid entry pressure	SGMD	Sweeping gas membrane distillation
MB	Methylene blue dye	SiO_2	Silica
MD	Membrane distillation	SVM	Support vector machine
MGMD	Material gap membrane distillation	TiO_2	Titanium dioxide

MO	Methyl orange dye	TP	Temperature polarization
PDMS	Polydimethylsiloxane	VMD	Vacuum membrane distillation
PEG	Polyethylene glycol	$Zn(CH_3CO_2)_2$	Zinc acetate

1. Introduction

Rapid progress of industrialization affects the water quality, resulting in an increasing freshwater crisis globally [1]. Inadequate treatment of wastewater leads to various chemical release to the environment, where large group of industrial waste contains dyes. These compounds are classified according to their chromophore structure, colour index (CI), and its application [2,3]. Classification of chromophore structure is based on functional groups of the dye molecule. This include acridine, anthraquinone, azo, cyanine, diarylmethane, indigoid, nitro, nitroso, oxazine, phthalein, quinone-imine, triarylmethane, triphenylmethane, xanthene [4,5]. On one hand, CI classification includes over 8000 synthetic dyes with various names used in industrial applications. Depending on the textile type, different dyes are commonly used, e.g., sulphur [6], reactive [7,8], cationic [2,9], and azoic dyes [10]. These dyes are used to colourize cotton, silk, wool, nylon, rayon, viscose, cellulose acetate, paper, polyester, leather, acrylic, and synthetic fibres. Owing to their extensive use in textile, pharmaceutics, rubber, paint, food, cosmetic, paper, and pulp industries, dyes are released to the water streams causing severe environmental pollution. Textiles processing require several steps, namely, bleaching, mercerization, printing, and finishing. These steps require large amount of water [11]. For instance, bleaching process

requires treatment with either reducing or oxidizing agents to get rid of the dye. In mercerization, the material is treated with specific chemicals to improve its strength and affinity to dyes. The finishing process towards the transformation of the fabrics into functional material like waterproofing, glazing, sizing, and smoothing generates huge quantities of wastewater containing dyes [12].

Despite wide use of dyes in many fields, they are known for their adverse health effect. Literature presented reported an increased cancer appearance linked to textile industry proximity [13,14]. Also, hairdressers exposed to oxidative hair dyes are diagnosed with respiratory health problems [15]. The release of dyes to the aquatic environment does not only affect human beings but also deteriorate water quality, affecting the level of dissolved oxygen. Moreover, dyes undergo chemical reactions exacerbating their environmental toxicity. Acute, chronic, or cytotoxic effect of dyes has been broadly reported in algae, bacteria, fish, and mice [16]. Other studies reported dye toxicity on brain, kidney, liver, heart, and other organs as well as respiratory, hormonal, and immune systems [17,18].

To minimize the adverse effects of dye wastewater, various physicochemical methods have been extensively used to treat it (**Figure 1**). Physical treatment processes include adsorption, ion exchange, and membrane technologies. These techniques are easy to use, economical, and chemical-free [19]. However, physical processes produce high amounts of sludge and are limited towards treatment of dye-containing wastewater. On one hand, various chemical processes including advanced oxidative processes (AOP), photocatalysis, and electrocoagulation have been extensively evaluated to treat the dye wastewater. Although they remove dyes from harsh operating conditions and generate less sludge, they are pH dependent, expensive and form undesirable by-products. Similarly, electrochemical processes produce no sludge and do not require use of chemicals. However, it is costly and less effective compared to other technologies.

Biological processes have also been used extensively to treat dye-containing wastewater. This involves enzyme, algae, yeast, bacterial, and fungal assisted processes [19]. Biological processes avoid chemical usage and produce no sludge. However, their efficiency is dependent on the water chemistry including pH fluctuations and other conditions inhibiting activity of the biological agents. The publication record (in the past 10 years since 2013) of the dye wastewater treatment is presented in **Figure 1a**. It is important to note that no single dye wastewater treatment process is the most suitable technology due to various advantages and drawbacks [20]. For instance, the complex nature of the dye wastewater hinders satisfactory treatments meeting regulatory standards upon use of the mentioned technologies. This necessitates the combination of various technologies towards production of high-quality water. However, membrane distillation (MD) emerged as a promising technology, capable of producing high-quality water from dye wastewater. The publication growth record of dye wastewater treatment through MD is presented in **Figure 1b**. The number of publications for dye wastewater treatment via all methods increased from 10,904 in 2013 to 46,884 in 2023. The total number of publications between 2013 and 2023 was 27,5431. This was a tremendous increase, indicating the research interests of this topic. In the case of dye wastewater treatment via MD, the publications increased from 677 in 2023 to 3,910 in 2023. The total number of publications between 2013 and 2023 was 21,105. Such developments demonstrate the capability of this technology in treating the dye-polluted wastewater.

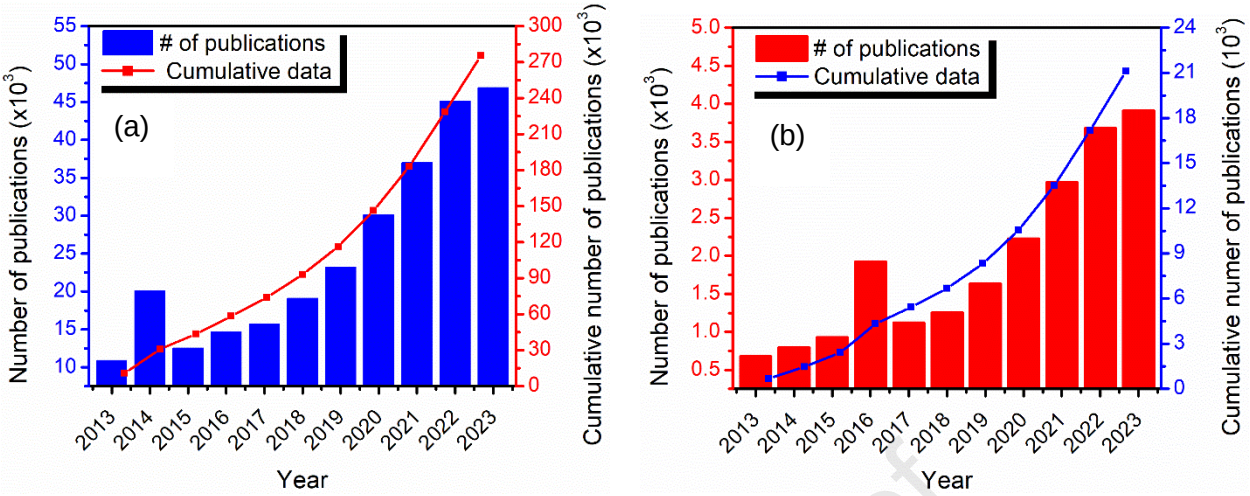

Figure 1: Number of publications related to dye wastewater treatment for the past ten years, (a) general treatment methods and (b) MD technologies. The data was retrieved from Scopus.

The first generation of MD research used commercially available hydrophobic membranes for wastewater treatment [21,22]. For example, the first report on the application of MD textile wastewater treatment date back in 1991, where the authors used commercial hollow fibre membranes made of polypropylene (PP) to treat synthetic wastewater by direct contact membrane distillation (DCMD) [23]. However, these membranes were not specifically fabricated for MD, thus presenting impaired performance as per reported permeate flux and energy efficiency. This is more challenging in case of textile wastewater treatment containing organic and inorganic dyes and other chemicals [24,25]. Therefore, the next generation of MD research for textile wastewater considered the fabrication of specific membranes for this application, particularly focusing on membrane fouling and operating conditions [26–29]. This involved employing hydrophobic polymers to produce wetting resistant membranes. The most studied polymers are polypropylene (PP), polyvinylidene fluoride (PVDF), polytetrafluoroethylene (PTFE), and polyethylene (PE) whose chemical structures are provided in **Figure 2**. The membranes prepared from these polymers are not wetted by process liquids, thus facilitating the mass transfer

through passage of the water vapour through the porous membrane. Other polymers evaluated in MD systems include HIPS and PDMS due to their hydrophobic nature. Although hydrophobic polymers presented fascinating results, they are increasingly modified to produce various novel polymer types for use in MD. These new generation of hydrophobic polymers are poly(ethene-co-chlorotrifluoroethene) (ECTFE), poly(vinylidene fluoride-co-tetrafluoroethylene) (PVDF-co-TFE), poly(vinylidene fluoride-co-tetrafluoroethylene) (PVDF-co-TFE), poly(vinylidene fluoride-co-chlorotrifluoroethylene) (PVDF-co-CTFE), and poly(tetrafluroethylene-co-hexafluoropropylene) (FEP) [30]. The membrane synthesis from these polymers is still at development stage of research, thus requiring intensive optimization process to improve the MD process performance. Among the first attempts, Mokhtar et al. (2014) fabricated PVDF hollow fibre membranes with varying polymer concentrations (12-18 wt%) for use in dye effluent treatment [31]. As per reported findings, 12 wt% polymer concentration, with 0.14 µm pore size and 450 kPa liquid entry pressure (LEP) provided excellent performance in terms of permeate flux (~5 $kg \cdot m^{-2}.h$) and dye rejection (>99.80%). Also, fouling behaviour of developed hollow fibre membrane was evaluated in a 40-h operation, presenting 50% flux decline [32].

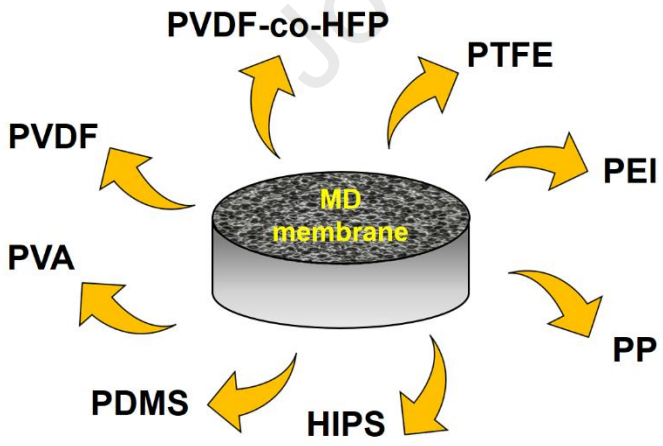

Figure 2: The commonly used polymers in MD processes

Despite progressive reports on MD applications towards treatment of dye effluents, there are limited review studies focusing on the subject matter. In their recent review study, Suresh et al. (2023) reported various membrane applications processes including adsorption, filtration, catalysis (oxidant activation, ozonation, Fenton process, and photocatalysis) and MD towards removal of synthetic dye from wastewater [33]. Besides dye treatment, MD is a viable technology for seawater desalination because it can process high-salinity water [34]. However, MD application is limited by low vapor flux and fouling – an inherent challenge in all membrane processes. One of the approaches to overcome these challenges is to make superhydrophobic membranes [35]. This this is achieved through the incorporation of inorganic nanomaterials such as graphene-based materials, carbon nanotubes (CNTs), metal-oxide nanoparticles (MNPs), clays as well as zeolitic imidazolate frameworks (ZIFs) [36,37]. Membrane wetting is another challenge associated with MD. Fouling and wetting in MD leads to immediate failure in membrane separation [38]. Therefore, it is important to understand fouling and wetting mechanisms in MD during treatment of various feed streams of different physicochemical properties [39]. The MD membranes are generally prepared from non-biodegradable polymers, harmful solvents and fluoroalkyl silanes. A recent review debates some inspiration for the fabrication of the next generation of MD membranes using greener approaches [40]. These membranes have potential for commercialization.

Some major drawbacks encountered with polymeric membranes is achieving high permeability and selectivity simultaneously [41]. Highly permeable membranes often have low permeability and vice versa. However, recent advancements have led to the formation of ultrathin membranes, breaking the trade-off between selectivity and permeance [42]. This is due to the ultrathin nature of the selective layer and lack of defects in the membrane structure. Several approaches including atomic layer deposition, in situ crystal formation, interfacial polymerization, Langmuir–Blodgett technique, facile filtration process, and gutter layer formation have been used to prepare

membranes with high selectivity and permeability. These procedures take advantage of the intrinsic nature of nanostructured materials such as polymers, zeolites, covalent–organic frameworks, metal–organic frameworks, and graphene to prepare membranes for various applications in liquid separation – a focus of this study. Detailed overview of these techniques can be found in the literature [43]. Chemical grafting or crosslinking of polyimide chains are other strategies adopted to improve selectivity and specific permeance. However, the separation efficiency often improves at the expense of fluid permeability as the degree of crosslinking increases [44]. Similarly, non-selective filler-polymer interfacial voids reduce selectivity of mixed matrix membranes [45].

Besides tremendous progress in the configuration of MD systems, there are many problems limiting its performance on a broad scale, requiring critical attention. The most challenging issues in addition to wetting and fouling affecting membrane flux and separation efficiency include high-energy consumption, long time of operation, and membrane regeneration. The current review reported different aspects and recent solutions in the effective MD process focusing on the main configurations used in laboratory and industrial scale, where considerable research articles focus on the commercial membranes. Although the MD is a promising technology, its effectiveness depends on several features including operation parameters like feed temperature, flowrate, feed concentration; physicochemical properties of the membrane (pore size and porosity, permeability, membrane thickness, hydrophobicity, thermal stability, polymer type used for membrane fabrication, and the MD system configuration. The current literature mainly tested MD setups in the laboratory scale suggesting a deep need for further optimization of membrane and module designs in near future, especially for textile wastewater treatment. There is a need to deliver customized high-porosity hydrophobic membrane design with the appropriate thickness and module configuration to reduce concentration and temperature polarization (CP and TP), minimize waste energy and increase MD efficiency and water recovery. More research should

optimize configurations and re-design the membranes by incorporating new materials (e.g. hollow fibres, nanofibres, and nanomaterials) to enhance the fluid dynamics, reduce waste energy, and improve re-use of membranes and versatility to deal with industrial dye effluents. To increase the operation scale of MD, more mitigation and cost-effective antifouling strategies should be implemented.

Among practical aspects, the theoretical studies are widely implemented to enhance MD technology. The artificial intelligence (AI)-based methods enable optimization of the input variables to achieve the highest efficiency of the dye removal (maximize the removal value). The key issue for developing efficient AI-based solutions is to provide the developers with large and good quality data. AI-based algorithms can increase the efficiency of the entire process, shortening its duration, optimizing its parameters, and reducing costs. Advanced machine learning techniques can support the development of the MD scale processes. However, this field of research is still poorly explored in textile wastewater treatment and need more modelling studies including correlation between the membrane and module design, and mechanism of fouling and wetting. These aspects are comprehensively and concisely addressed in this review, with the strategy of ensuring improved MD process performance in textile industry.

2. Membrane development for textile and dye wastewater treatment

Membrane development characterized by fouling and scaling resistance is a promising approach towards treatment of dye wastewater in MD. For example, An et al. (2017) fabricated a novel nanofibre membrane by incorporating polydimethylsiloxane (PDMS) onto a electrospun poly(vinylidene fluoride-co-hexafluoropropene) (PVDF-HFP) membrane [46]. The new hybrid membrane exhibited a notable decrease in surface energy, as seen by the contact angle measurement of 155.4°. Additionally, the membrane displayed high surface roughness (R_a = 1285

nm). The zeta potential of the new membrane exhibited a more pronounced negative value compared to a commercial PVDF membrane. As per authors argument, the new membrane exhibited wetting resistance and antifouling qualities during treatment of dye wastewater with varying charges. This resulted in the formation of a flake-like structure of dye-dye interactions on the surface of the membrane, rather than within its pores. Furthermore, this phenomenon resulted in a notable increase in the productivity of the new nanofibre membrane, reaching a permeate flux of 34 $L \cdot m^{-2} \cdot h^{-1}$, which is 50% greater compared to the productivity of the commercial membrane.

Pore wetting is another major challenge of MD, demonstrating a direct collapse of the membrane performance [47]. During treatment of textile wastewater, chemicals and surfactants increase the pore wetting risk [48]. García et al. (2018) used a custom-made PTFE membrane coated by hydrophilic polyurethane (PU) in a pilot scale DCMD system [49]. The system was developed to treat textile wastewater containing surfactant. Authors reported increased wetting of the commercial PTFE membrane as evidenced by increase in the permeate conductivity. In contrast, the hydrophilic-coated membrane exhibited a consistent decrease in permeate conductivity, indicating the presence of a wetted membrane. Despite the favorable outcome, the coated membrane did not withstand a routine cleaning procedure including washing by sodium hydroxide (NaOH), which is commonly employed in membrane processes.

Similar to other properties, MD performance is affected by membrane porosity. In fact, high porosity is required to transfer the vapour molecules. This achieved by new fabrication techniques for highly porous, flat sheet membranes, such as electrospinning [50,51]. Shirazi et al. (2020) developed a durable membrane with a dual-layer structure and exceptional characteristics for treatment of industrial dye wastewater [52]. This nanofibre membrane possessed a composite structure consisting of the cost-effective styrene acrylonitrile (SAN) polymer as the top layer,

alongside a commercially available hydrophilic nonwoven material for the supporting layer. As per reported findings, the approach presented potential commercialization of the DCMD process in the treatment of high-temperature dye wastewater. The nanofibre membrane exhibited notable characteristics compared to a commercial PTFE membrane, including a high hydrophobicity (≥148°), increased porosity (≥81%), and a reduced tortuosity factor (1.71). All these led to a superior performance of membrane, precisely, 28.31 $kg \cdot m^{-2} \cdot h^{-1}$ permeate flux and a commendable rejection rate of 98.2%. In their study, Khoshnevisan and Bazgir (2020) examined a hot-pressed nanofibre membrane made of HIPS towards treatment of textile wastewater at different concentrations [52]. The hot-press post treatment of the membrane samples enhanced mechanical strength with an improvement in pore size distribution and LEP. The dye rejection of the DCMD process exceeded 99.8% when varying amounts of dye were utilized as the feed. However, the membranes were fouled at high dye concentrations. Yadav et al. (2021) developed an innovative mixed matrix membranes, including MIL101(Fe) impregnated into PVDF-HFP [53]. The membrane composed of 20% PVDF-HFP and 0.5% MIL101(Fe) presented >98% dye removal along with 6.75 $L \cdot m^{-2} \cdot h^{-1}$ permeate flux.

Photocatalytic MD membranes emerged as a promising self-healing to improve process performance. For example, Huang et al. (2017) fabricated photocatalytic membrane with highly porous structure by sintering electrospun composite membranes consisting of PTFE, poly(vinylalcohol) (PVA), and zinc acetate ($Zn(CH_3CO_2)_2$) [54]. The resulting membranes were supported by a substrate of zinc oxide (ZnO). According to the findings, the spinning solution displayed favorable electrospinning characteristics, while the membranes exhibited remarkable flexibility, elevated chemical stability, and large specific surface area. The authors applied their PTFE/ZnO membranes in vacuum membrane distillation (VMD) through the implementation of photo-degradation tests towards efficiency evaluation. According to the obtained results, the trials using photo-degradation yielded a notable 99.7% salt rejection. In addition, the PTFE/ZnO

membranes exhibited favorable self-cleaning capabilities. According to reported findings, the used membranes presented 94.1% flux recovery following a 3-h period of UV irradiation cleaning (**Figure 3**).

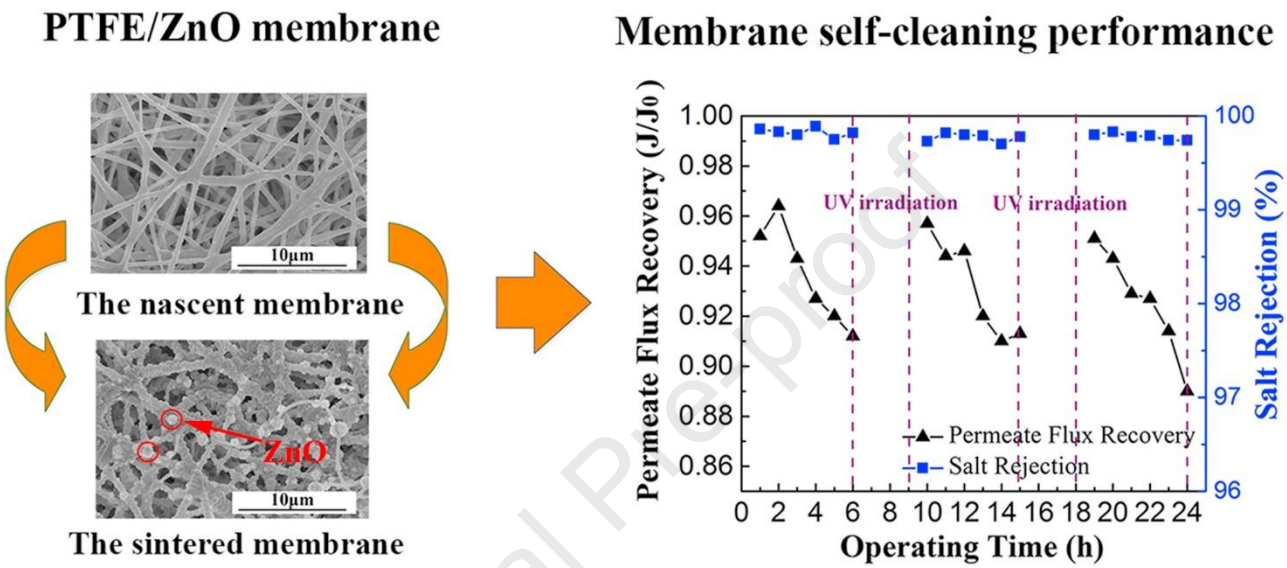

Figure 3. The nanofibre PTFE/ZnO porous membrane with a self-cleaning mechanism for dye removal by VMD [55].

In addition to flat sheet membranes, research is geared towards preparation of hollow fibre membranes for textile wastewater treatment. Li et al. (2019) used the dilute solution coating technique to manufacture hydrophobic PVDF hollow fibre composite membranes [56]. The process was aimed at fabricating a specific surface structure analogous to the dual micro-nano structure, mimicking the properties of a lotus leave. This preparation procedure increased the surface contact angle of the membrane from 93.6° to 130.8°. The fabricated membranes were evaluated towards separation of congo red and methylene blue dyes from synthesized wastewater using VMD. The findings reported an increase in permeate flux and dye rejection

(>99%) in comparison with the control PVDF membrane. In another work, Mousavi et al. (2021) modified a hydrophobic polyetherimide (PEI) hollow fibre membrane through a dip-coating technique [57]. The authors coated the membranes using 2-(perfluoroalkyl) ethanol (Zonyl® BA). The prepared membranes were evaluated to remove methylene blue from a synthesized wastewater stream via air gap membrane distillation (AGMD). During a 76-h experiment, the developed hollow fibre membrane exhibited a permeate flux of 6.5 $kg \cdot m^{-2} \cdot h^{-1}$ and a methylene blue rejection of 98%.

In a recent work, Xie et al. (2023) fabricated a superhydrophobic PVDF membrane using a spray-coating technique with fluorinated silica nanoparticles (SiO_2 NPs) (**Figure 4**) for the treatment of saline dye wastewater [58]. The authors performed a detailed investigation on the effects of various operating variables (i.e., temperature difference, feed flowrate, salt concentration, dye concentration, and dye species) in DCMD. According to the research findings, the prepared superhydrophobic membrane presented a remarkable resistance to wetting and fouling with 99.9% salt and dye rejection. Additionally, the superhydrophobic membrane exhibited a notable water recovery rate of 90%. However, the authors reported a marginal 13.4% decrease in the permeate flux during a 39-h DCMD evaluation.

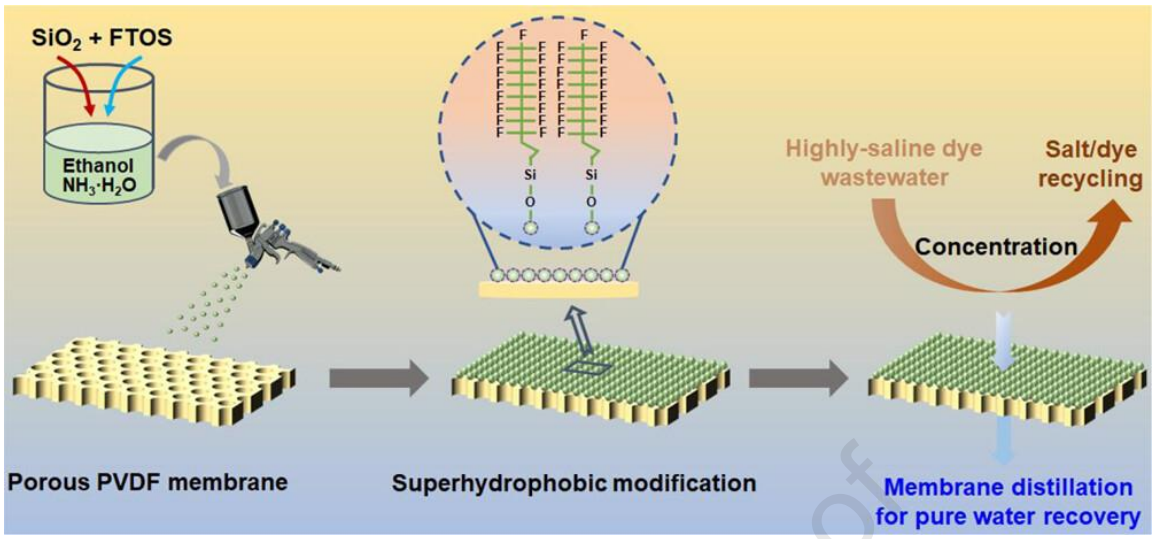

Figure 4. Procedural fabrication of superhydrophobic SiO_2/PVDF membrane for dye removal from a highly saline wastewater [58].

In the preparation of polymer-based ultrafiltration (UF)/nanofiltration (NF) membranes for MD, recent trends adopted greener approaches involving utilization of green solvents in membrane fabrication. Various polymeric membranes have been prepared via these green synthesis methods, and they include porous Matrimid® 5218 membranes [59] and NF membranes based on polyamide-cellulose acetate [60]. Similarly, the preparation of green nanofillers and their incorporation into polymeric NF membranes has been reported. A recent comprehensive review discusses recent and ongoing progress on novel nanocomposite membranes based on green approaches for heavy metals removal from water [61]. The membranes with green nanofillers improved hydrophilicity, water permeability and pollutant rejection capability. These membranes present fouling resistance and can be used for a lengthy period without degradation.

Table 1 provides a summary of the MD application towards dye removal from textile effluents. Among the MD configurations, the most popular design is DCMD owing to its simplicity in setup and low capital cost [17]. In DCMD, both the feed and permeate solutions are in direct contact with the membrane at different interfaces. The temperature difference between the two membrane interfaces creates a partial vapour, facilitating the mass transfer from the feed to the permeate. Although the DCMD is known to be simple to design and operate, it experiences high conductive heat loss and thermal energy inefficiencies [62]. To minimize the heat loss in MD processes, the VMD was proposed. In this configuration, the membrane is placed between the hot feed and the vacuum chamber [63]. The water vapour condensers outside the module in an external condenser. Although the VMD is thermally efficient, it is affected by membrane wetting due to high pressure differences resulting in low separation efficiencies [64]. Similarly, the cold inert gas is used to sweep the water vapour from to the external condenser, giving rise to SGMD. This configuration is thermally efficient [65]. However, it requires large condensers, thus making it expensive. In addition to SGMD, the AGMD was introduced, presenting high thermal efficiency influenced by reduced heat loss. In this configuration, the membrane is placed between the hot feed solution and the stagnant air [51]. The water vapour passes through the porous membrane and stagnant air to the condensing plate. This configuration faces mass transfer resistance resulting in low permeate flux [62]. All these configurations require hydrophobic membranes to operate effectively. Commonly used membrane materials for MD processes are PTFE, PVDF, and PP. The choice of these polymeric materials involves their outstanding properties namely, high hydrophobicity, low surface energy, low melting point, high tolerance to oxidizing agents, and good thermal stability [18]. From **Table 1**, dyes such as reactive orange, reactive blue, reactive black, methylene blue, and congo red are commonly used to evaluate the performance of membrane during MD processes with the operating feed and permeate temperatures 40-80°C

and 10-20°C, respectively. As per reported findings, the permeate flux deteriorated as a function of time, mainly due to the surface fouling caused by dye adsorption/deposition.

333 **Table 1**. Applications of MD process for the removal of dyes from textile effluent

Membrane materials	**MD configuration**	**[a]Operating Parameter**	**Dye/concentration**	**[b]Flux**	**Ref**
High-impact polystyrene (HIPS) and styrene-acrylonitrile (SAN4)	DCMD	T_f = 52 ± 2 °C T_p = 12 ± 3 °C Q_f = 0.24 L·min^{-1} Q_p = 0.48 L·min^{-1}	2,000 mg·L^{-1} reactive orange-122 2,000 mg·L^{-1} disperse red-60	Reactive Orange-122 J_i = 38.77 kg·m^{-2}·h^{-1} J_f = 35.29 kg·m^{-2}·h^{-1} T = 6 h Disperse Red-60 J_i = 36.33 kg·m^{-2}·h^{-1} J_f = 23.40 kg·m^{-2}·h^{-1} T = 6 h	[43]
Polytetrafluoroethylene (PTFE)	DCMD	T_f = 60 °C T_p = 20 °C	400 mg·L^{-1} reactive blue	Reactive blue dye J_i = 3.33 kg·m^{-2}·h^{-1} J_f = 3.40 kg·m^{-2}·h^{-1} T = 7 h	[25], [44]
Polyetherimide (PEI) membranes and	SGMD	T_f = 60 °C T_p = 20 °C	1,000 mg·L^{-1} methylene blue	Methylene blue (pristine PEI) J_i = 24.17 kg·m^{-2}·h^{-1}	[25]

modified by polydimethylsiloxane (PDMS)		Q_f = 0.20 L·min^{-1} Q_p = 0.10 L·min^{-1}		J_f = 13.96 kg·m^{-2}·h^{-1} T = 130 h Methylene blue (PEI with PDMS) J_i = 21.88 kg·m^{-2}·h^{-1} J_f = 17.71 kg·m^{-2}·h^{-1} T = 130 h	
Poly(tetrafluoroethylene) (PTFE)	DCMD	T_f = 60 °C T_p = 20 °C Q_f = 1.5 L·min^{-1} Q_p = 0.5 L·min^{-1}	1,000 mg·L^{-1} reactive black 1,000 mg·L^{-1} disperse black	Reactive black J_i = 14.46 kg·m^{-2}·h^{-1} J_f = 10.89 kg·m^{-2}·h^{-1} T = 4 h Disperse black J_i = 11.43 kg·m^{-2}·h^{-1} J_f = 6.52 kg·m^{-2}·h^{-1} T = 4 h	[5], [45]
Poly(tetrafluoroethylene) (PTFE) with	DCMD	T_f = 60 °C T_p = 20 °C Q_f = 0.5 L·min^{-1}	100 mg·L^{-1} congo red	Congo red J_i = 28.10 kg·m^{-2}·h^{-1} J_f = 14.20 kg·m^{-2}·h^{-1}	[5]

polypropylene (PP) support layer		Q_p = 0.5 L·min^{-1}		T = 24 h	
Polyvinylidene fluoride (PVDF)	DCMD	T_f = 70 °C T_p = 20 °C	7 mg·L^{-1} maxilon blue 5G 7 mg·L^{-1} drimarene yellow K-2R 7 mg·L^{-1} sodium fluorescein	Maxilon blue 5G J_i = 21.80 kg·m^{-2}·h^{-1} J_f = 18.62 kg·m^{-2}·h^{-1} T = 47 h Drimarene yellow K-2R J_i = 21.20 kg·m^{-2}·h^{-1} J_f = 20.04 kg·m^{-2}·h^{-1} T = 47 h Sodium fluorescein J_i = 21.70 kg·m^{-2}·h^{-1} J_f = 19.35 kg·m^{-2}·h^{-1} T = 47 h	[19]
Poly(tetrafluoroethylene) (PTFE)	AGMD	T_f = 60 °C T_p = 20 °C Q_f = 0.38 L·min^{-1} Q_p = 0.60 L·min^{-1}	100 mg·L^{-1} textile wastewater mixtures of sodium chloride with sunset yellow	Sodium chloride with sunset yellow J_i = 12.36 kg·m^{-2}·h^{-1} J_f = 12.00 kg·m^{-2}·h^{-1}	[46]

			100 mg·L^{-1} rose bengal	T = 20 h Sodium chloride with rose Bengal J_i = 10.27 kg·m^{-2}·h^{-1} J_f = 9.82 kg·m^{-2}·h^{-1} T = 20 h	
Poly(tetrafluoroethylene) (PTFE)	DCMD	T_f = 60 °C T_p = 20 °C Q_f = 1.5 L·min^{-1} Q_p = 0.5 L·min^{-1}	30 mg·L^{-1} reactive black 30 mg·L^{-1} disperse black	Reactive black J_i = 18.55 kg·m^{-2}·h^{-1} J_f = 13.68 kg·m^{-2}·h^{-1} T = 24 h Disperse black J_i = 22.37 kg·m^{-2}·h^{-1} J_f = 18.42 kg·m^{-2}·h^{-1} T = 24 h	[47]

Poly(tetrafluoroethylene) (PTFE) with polypropylene (PP) support layer	DCMD	T_f = 60 °C T_p = 20 °C Q_f = 0.5 L·min^{-1} Q_p = 0.5 L·min^{-1}	500 mg·L^{-1} congo red	Congo red J_i = 34.23 kg·m^{-2}·h^{-1} J_f = 12.50 kg·m^{-2}·h^{-1} T = 24 h	[48]
PVDF-co-hexafluoropropylene (PVDF-co-HFP)	DCMD	T_f = 50 °C T_p = 7 °C Q_f = 1.8 L·min^{-1} Q_p = 1.8 L·min^{-1}	100 mg·L^{-1} methylene blue (MB) 100 mg·L^{-1} congo red + 4% NaCl	Methylene blue, congo red and NaCl J_i = 5.10 kg·m^{-2}·h^{-1} J_f = 3.40 kg·m^{-2}·h^{-1} T = 6 h	[32]

[a]Feed temperature: T_f, Feed flowrate: Q_f, Permeate temperature: T_p. Feed permeate: Q_p,

[b]Initial flux: J_i, Final flux: J_f, Sampling time: T

3. Membrane fouling in textile/cosmetic wastewater

Fouling remains a major drawback in the application of membranes in liquid separations [66]. Fouling does not only deteriorate membrane performance, but also increases operational costs due to requirements of frequent cleaning and membrane replacement [67]. Membrane fouling is governed by various factors [68]. Various strategies are adopted to alleviate fouling in hydraulic- (NF/RO), osmotic- (FO) and vapour-pressure (MD) driven membranes [38]. Some of the strategies used to prevent fouling include the incorporation of nanofillers to prepare high performance and stable membranes [69,70]. Nanofiller addition increases electron donor or Lewis base components of the membranes, thus reducing membrane-foulant affinity interactions [71]. Subsequently, reversible fouling ratio contributes more to the observed total fouling ratio [69,71]. Other modification processes include polymer blending, nanocomposite materials and chemical modification [72]. Also, alternative novel approaches used to combat biofouling include the addition of bacteriophages as biocidal agents, quorum quenching, advanced oxidation processes, and addition of metazoans amongst others [73].

Inorganic dyes present in textile and cosmetic wastewater can potential cause membrane fouling of MD systems. During the MD process, only water molecules (vapour) pass through the hydrophobic membrane while non-volatile dye molecules are rejected by the membrane. As a result, the dye concentration adjacent to the membrane surface is gradually increased, causing concentration polarization (CP) [74]. Furthermore, high dye concentrations near the membrane surface develop a cake layer, leading to a significant increase in membrane transport resistance and reduction in permeate flux. By increasing the dye concentration in the feed solution from 50 ppm to 1,000 ppm, Mokhtar et al. (2015) reported a gradual decline in permeate flux from ~10

360 $kg \cdot m^{-2} \cdot h^{-1}$ to 6.5 $kg \cdot m^{-2} \cdot h^{-1}$ when tested under hot and cold solution temperature of 70 °C and 20
361 °C, respectively [75]. The flux decline at high solute concentration is mainly caused by the lower
362 water vapour transport rate, i.e., lower activity coefficient of water vapour pressure. Furthermore,
363 high concentration of dye increases the attachment of dye particles on the membrane surface,
364 causing a partial or full pore blockage.

365 Membrane fouling involves pore blockage and aggressive formation of a cake layer, typically
366 induced by the interaction between the membrane, the solutes in solution and operating
367 conditions. Fouling takes place through various mechanisms, typically (a) complete blocking, (b)
368 standard blocking, (c) intermediate blocking, and (d) cake filtration (**Figure 5a**) [76]. In compete
369 blocking, the solutes seal all the membrane pores. In standard blocking, the solutes are adsorbed
370 or deposited within the membrane pores [77]. The continuous accumulation of the particles within
371 the membrane pores increases the size of the foulant, ultimately causing complete pore clogging.
372 In intermediate blocking, the particles form an accumulative layer on the surface of the membrane.
373 Meanwhile, the combination of this layer, presence of coordinating metals and CP establishes a
374 cake layer, resulting in cake filtration [78]. Membrane fouling of MD processes is a complex
375 phenomenon requiring an understanding of the parameters affecting it to establish its
376 mechanisms. Fouling is affected by various factors namely, (a) membrane properties including
377 hydrophobicity, pore size, roughness, surface charge, functional groups, (b) feed water chemistry
378 including solubility, diffusivity, hydrophobicity, pH, ion strength, type of foulant, and (c) operating
379 conditions such as flow velocity, processing temperature, and transmembrane pressure (TMP).

380 The identity of the membrane fouling is dependent on feed water, foulant characteristics, and
381 different membrane properties. Typically, hydrophobic membranes foul more compared to
382 hydrophilic membranes. Also, membrane roughness causes excessive fouling due to air
383 entrapment which promotes the fluid drop on the surface of the membrane. According to DLVO
384 theory, the membrane-foulant and foulant-foulant interactions are described by the van der Waal,

385 electrical and acid-base interactions (**Figure 5b**) [76]. Briefly, the foulants of opposite charges will
386 interact electrostatically. The electrostatic interaction can be attractive or repulsive depending on
387 the direction of the membrane-foulant charges. Also, depending on the membrane and foulant
388 properties, hydrophobic-hydrophobic interactions occur, which is often difficult to break.
389 Submerging of the membrane in water disturb the hydrogen bonds of the molecule, which in turn
390 increase the membrane surface free energy. Upon interaction with the foulant, the high surface
391 energy promotes fouling. In the presence of metal ions, the covalent interaction takes place
392 through metal-organic complexation [79]. For instance, the multivalent ions such as calcium form
393 bridged complexes between the membrane surface and carboxylic groups present on the foulant.

394

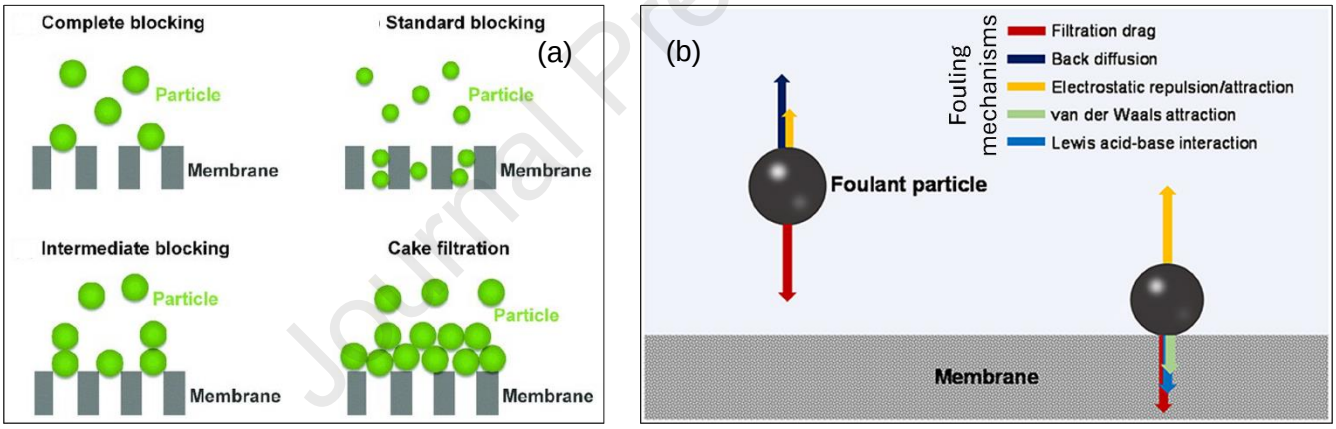

395

396 **Figure 5**: Schematic illustration of (a) pore blocking causing mass transfer resistance and (b)
397 membrane fouling mechanisms [76,79].

398

399 Since the pressure difference across the membrane during MD process is minimal, the formation
400 of the cake layer due to dye deposition is significantly slower compared to the pressure-driven
401 membrane processes such as NF and reverse osmosis (RO) [66,80]. Ramlow et al. (2020)
402 evaluated the performance of PTFE membrane for textile wastewater treatment using DCMD

process [81]. Reportedly, the membrane performance declined moderately from 28.68 to 19.47 $kg \cdot m^{-2} \cdot h^{-1}$ over the sampling time due to the accumulation of foulants on the membrane surface. Although the deposited dyes could be effectively removed from the membrane via physical and/or chemical cleaning, the presence of surfactants in the wastewater react chemically with the dyes, making flux recovery process difficult. Using PTFE membrane for textile wastewater treatment via DCMD process, Fortunato et al. (2021) reported a strong inverse correlation between the membrane fouling layer and the normalized membrane vapour flux [82]. The authors attributed this phenomenon to the cake-enhanced temperature polarization (CETP). As the feed temperature increased, the flux was decreased due to the increased foulant deposition. Therefore, MD operation with low feed temperatures (40–60 °C) is imperative to minimize membrane surface fouling. The hydrophobic nature of textile and cosmetic industry dyes increases the rate of their adsorption on the hydrophobic membrane.

Dye molecules adsorb onto the membrane surface due to attractive forces such as van der Waals, hydrogen bonding, and electrostatic interactions. Once adsorbed, the dyes form a blocking layer on the pores and hinders water flow [83]. Adsorption of dye onto the membrane surface is influenced by process conditions (e.g., dye concentration, solution pH, solution temperature, and contact time) and membrane characteristics (e.g., degree of hydrophobicity, pore size distribution, porosity, and charge) [84]. Among other factors, pH plays an important role in adsorption, with high affinity of cationic dyes due to their negative surface charges, while anionic dyes with positive surface charges present high affinity to membrane surfaces. Cationic dye adsorption is favoured at pH values greater pH point of zero charge (pHpzc), whereas anionic dye adsorption is favoured at pH values lower than pHpzc [85].

Additionally, the dye concentration affects the adsorption capacity onto the membrane. At the early stage of dye attachment, adsorption rate increases with the increase in dye concentration. Upon saturation, the adsorption rate decreases due to the repulsion between the adsorbed dye

molecules. On the other hand, the adsorption capacity increases at high temperatures following the increase in the mobility of dye molecules [86]. Similarly, the membrane pore size influence the dye adsorption efficiency, with dye molecules absorbing into large pore size [87]. The typical pore sizes of MD membranes suitable for dye removal range from 0.2 to1.0 μm [88,89]. In addition to pore size, liquid entry pressure of membranes should be 1.2, 3.1 and 3.6 bar for PP, PVDF, and PTFE membrane, respectively to prevent the penetration of liquid into membrane pores in textile wastewater treatment [90].

Some common dyes react chemically with the membrane through the formation of single or multi-chelates, creating complexes, and oxidation-reduction-absorbance reactions [91]. Furthermore, the membrane pores accelerate interactions between the dye molecules and the membrane through hydrogen bonding, thus contributing to dye adsorption. The dye molecules, with sulfonic groups and aromatic rings, exhibit strong electrostatic interactions and π-π stacking with the spongy materials. Hydrogen bonding further reinforces this interaction [77]. **Table 2** presents the mechanism of fouling comparing different types of dyes described in the recent literature.

Table 2. Types of dye vs. mechanism of interactions with the membranes during MD processes

Membrane type	Dye	Classification of dye	Mechanism	Ref.
DCMD	Congo red	azo dye/ anionic	hydrophobic interactions between the surface of the membrane and dye molecules;	[92]

MD	Methylene blue	azo dye/ cationic	electrostatic interaction (EI) and π-π conjugation	[93]
VMD	Methylene blue	azo dye/ cationic	surface adsorption	[94]
DCMD	Acid Red 18	azo dye/ anodic		[95]
MD	Direct Blue 6	azo dye/ cationic		[95]
MD	Malachite green	azo dye/ cationic	surface adsorption	[96]
DCMD	Methylene blue	azo dye/ cationic	not specified	[97]
MD	Direct blue 53 and Acid black 1	azo dye/anionic	electrostatic interactions, surface adsorption	[87]
MD	Acid red 87, Azure A, Basic blue	azo dye/cationic	electrostatic interactions, surface adsorption	[87]

DCMD	methylene blue, crystal violet13	azo dye/cationic	electrostatic interactions, surface adsorption	[98]
DCMD	acid red 18, and acid yellow 36	azo dye/anionic	electrostatic interactions, surface adsorption	[98]
MD	reactive yellow, reactive red, reactive blue, and reactive black	reactive dyes	electrostatic interactions, van der Waals forces, dye aggregates formation onto membrane surface	[99]
MD	disperse yellow, disperse red, disperse blue, and disperse black	disperse dyes	electrostatic interactions, van der Waals forces, dye aggregates formation onto membrane surface	[99]

444

445

446 3.1. Effects of fouling on process performance

The presence of the dye molecules on the membrane surface or within pores adversely affect the membrane hydrophobicity and its antiwetting properties. Previous study analysed the fouling conditions caused by dye molecules via optical coherence tomography (OCT) scanning (**Figure 6a**) [82]. According to the reported findings, the perpendicular feed flow increased the thickness of fouling layers along the membrane length (**Figure 6b**). Fouling form a resistant layer on the membrane surface, promoting a mass transfer resistance [100]. Persistent development of fouling layer cause excessive flux decline, with an ultimate degradation of the MD process performance [101]. **Figure 6c** presents the cross-sectional structure and the inner surface field emission electron scanning microscope (FESEM) images of the fouled membrane after a 40-h treatment of industrial textile wastewater [101]. The inner structure of membrane was severely covered by dye particles altering its surface characteristics and causing remarkable flux decline (**Figure 6d**).

According to Fortunato et al. (2021), flux decline is directly related to the fouling layer on the membrane (R^2: ~0.96) [82]. Although the process can be increased by operating at higher feed temperatures, such approach is associated with several negative challenges, degrading both the membrane and the flux. Exposing the membrane to high temperatures for extended periods reduce their lifespan due to material damage. The high thermal stress cause changes in the membrane material, such as loss of hydrophobicity, changes in pore size and structural damage, ultimately decreasing the membrane's efficiency and performance. Additionally, at high operating temperatures, the CP is more pronounced. It occurs when solutes in the feed solution accumulate near the membrane surface, creating a concentration gradient and hinderance of water vapour transport [102]. Additionally, high operating temperature difference increases energy consumption, thus making MD process costly compared to the pressure-driven membrane processes.

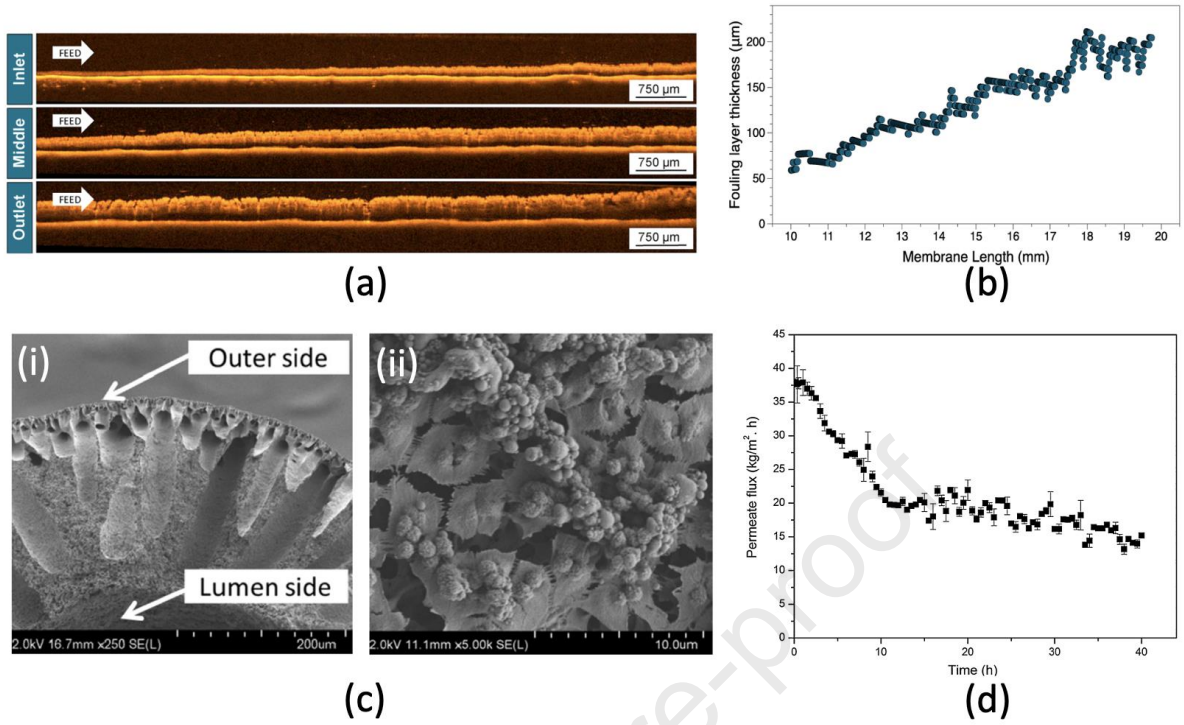

Figure 6. (a) OCT scan of fouling characteristics at inlet, middle and outlet positions on the membrane surface after 24-h sampling time (feed flow at perpendicular direction) via MD process and (b) Thickness of fouling layer along the membrane length (Testing conditions: temperatures of feed and permeate at 60 °C and 20 °C, respectively, cross-flow velocities of feed and permeate stream at 0.14 $m \cdot s^{-1}$ [82]. (c) FESEM images of Cloisite 15A-modified PVDF hollow fibre membrane used for industrial textile wastewater treatment, (i) Partial view of the membrane structure and (ii) accumulation of dye molecules in the inner surface of the membrane and (d) permeate flux as a function of time (Testing conditions: feed and permeate temperatures at 90 °C and 25 °C, respectively, feed and permeate cross-flow velocities of at 0.023 $m \cdot s^{-1}$ and 0.002 $m \cdot s^{-1}$, respectively and hot feed solution flowing through membrane lumen) [32].

In addition to flux decline, fouling induce physical damage of the membrane [103]. These include changes in pore structure, size distribution and decreased mechanical strength [104]. Consequently, membrane resistance to wetting is reduced, thus compromising dye separation

efficiency and distillate quality [105]. Mousavi et al. (2021) reported a decrease in methylene blue rejection for both the PEI and PEI-PDMS membranes during 120-h MD experiment [106]. Reduced dye rejection was associated with membrane pore wetting.

Also, fouling affects the overall economic cost of MD treatment plants, and therefore requires a critical attention. To restore process efficiency after fouling, periodic cleaning is carried out, thus increasing the process operational costs. According to Adel et al. (2022), membrane cleaning should be conducted immediately when the flux drops below 10% to prevent irreversible fouling [107]. Nevertheless, frequent cleaning (particularly involving chemical agents) promotes downtime and affect membrane structure which ultimately impact the overall operating cost.

3.2. Fouling control strategies

3.2.1. Membrane materials development

The development of advanced membrane materials has been extensively explored as an effective strategy to reduce fouling in MD dye treatment processes. The accumulation of dye molecules and other foulants on the membrane surface hinders the MD process, reducing membrane flux, and compromising separation efficiency [108]. Hydrophilic coatings, such as SAN, PVA, polyethylene glycol (PEG), CNTs, and silver nanoparticles (AgNPs) have been previously used to modify membrane surface to increase their surface hydrophilicity [109–112]. Hydrophilic coatings play a significant role in reducing dye fouling in MD. It creates a strong affinity for water molecules, establishing a repelling barrier. This reduces the attachment of dye molecules on the membrane, thus minimizing fouling. Additionally, the coatings promote self-cleaning of the membrane surface. When water vapour condenses on the hydrophilic surface, it forms a thin water film capable of detaching the foulants from the membrane. Zwitterionic polymers, characterized by positive and negative charges demonstrated excellent anti-fouling properties

[113]. When grafted onto the membrane surface, these polymers create a repulsive force against dye molecules and foulants, preventing their attachment to the membrane [113]. **Figure 7a** illustrates the improved surface properties of PVDF membrane in reducing the affinity of dye molecules and foulants on the membrane surface, aiming to mitigate fouling and improve flux [114]. Huang et al. (2023) deposited multiple layers of sulfobetaine methacrylate (SBMA) and acrylic acid (AA) on a hydrophobic PVDF membrane using the layer by layer (LbL) polyelectrolyte deposition technique to produce the wetting and fouling-resistant membrane [114]. Although coating improved membrane resistance to flux decay, it reduced the membrane pore sizes, thus minimizing the initial permeate flux of the process (**Figure 7b**). Shirazi et al. (2020) developed a dual-layer, hydrophobic/hydrophilic SAN4-HIPS membrane embedded with microspheres through a gas-assisted electrospinning technique [115]. This novel nanofibrous membrane was evaluated for its efficiency in treating hot dyeing effluent using DCMD [115]. The membrane exhibited desirable properties, such as high permeate flux of 28.31 $kg \cdot m^{-2} \cdot h^{-1}$ with a 99% dye rejection. Also, the membrane presented excellent resistance to pore wetting throughout 50-h dye wastewater treatment (**Figure 7c**). Photocatalytic nanoparticles embedded onto the membrane degrade dye molecules under UV irradiation [116]. This self-healing mechanism helps to maintain a clean membrane surface and reduce fouling. Yadav et al. (2021) successfully fabricated membranes with UV-cleaning properties by integrating porous titanium dioxide (TiO_2) into the PVDF-co-HFP membrane [117]. The TiO_2 NPs were synthesized using controllable large-scale synthesis protocols involving spray drying followed by calcination. In this study, a membrane incorporating 3 wt% TiO_2 NPs demonstrated ~100% dye removal efficiency for MB and CR. Although the membrane flux was reduced as a function of time, a stable flux was attained during the first 50-h operation (**Figure 7d**). Furthermore, the DCMD experiments presented a remarkable 91% flux recovery rate after 4-h UV-cleaning.

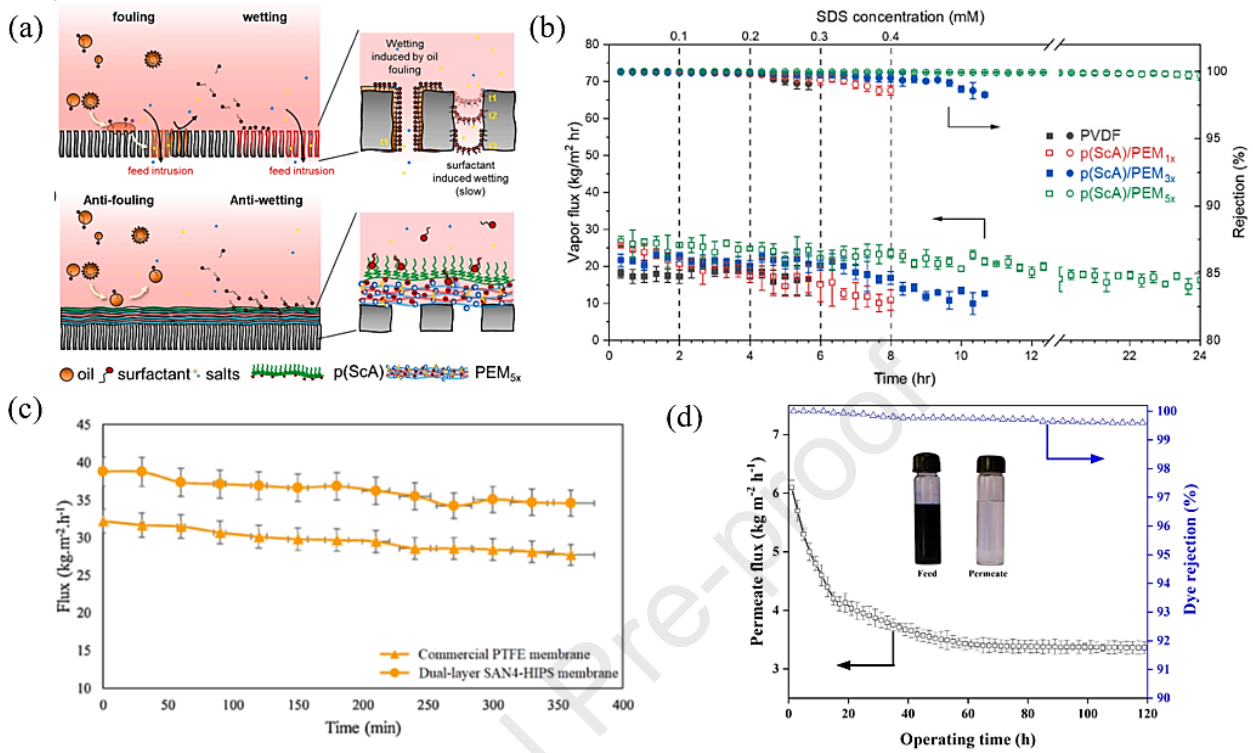

Figure 7: (a) Fouling of the pristine and hydrophilic-coated membrane [114] and (b) Permeate flux and rejection of the hydrophilic-coated membrane during MD process (feed solution: 3.5 wt% NaCl) [114]. (c) Permeate flux of dual-layer SAN4-HIPS membrane and commercial PTFE membrane during treatment of reactive orange-122 dye wastewater using DCMD (Testing conditions: temperatures difference of feed and permeate: 53 °C, feed and permeate flowrate were set at 0.48 L·min^{-1} and 0.24 L·min^{-1}, respectively and hot feed solution flowing through membrane lumen) [115]. (d) Permeate flux and dye rejection of 3 wt% TiO_2-modified PVDF-co-HFP matrix membrane during DCMD process [117].

3.2.2. Process control

The MD operates based on thermal principles, with its flux performance relying heavily on water vapour transfer across the membrane. However, accumulation of scalants and foulants on the membrane surface decreases the vapour pressure, resulting in a permeate flux decline. Thus, effective control of operating parameters, especially vapour pressure and feed temperatures are crucial in maintaining optimal flux output in the presence of foulants [118]. The Antoine equation **(Equation 1)** governs the relationship between the vapour pressure and the feed temperature. This equation describes the heat and mass transfer phenomena in MD process. The high vapour pressure and the permeate flux are attained at high feed temperatures. Besides improving permeate flux [118], elevated feed temperatures reduce TP, leading to enhanced mass transfer across the membrane [119]. Criscuoli et al. (2008) conducted an experimental study to remove Remazol Brilliant Blue R dye using VMD process. The results presented a two-fold increase in flux from 27.5 to 57 $kg \cdot m^{-2} \cdot h^{-1}$ upon increase in feed temperature from 40 °C to 60 °C [120].

$$\log_{10}(p) = A - \frac{B}{C+T} \quad [1]$$

where p is the absolute vapour pressure, T is the temperature (in Celsius) and A, B, and C are Antoine coefficients specific to the substance.

Besides optimizing the feed temperature alone, Hickenbottom and Cath (2014) investigated temperature and flow reversal techniques as novel approaches to effectively mitigate fouling in MD process and restore flux and salt rejection [121]. In the flow reversal method, the feed side and the permeate side channels were reversed (i.e., the feed side becoming the permeate side and vice versa). The temperature reversal method utilizes a cyclic process where a cold feed stream is circulated without heating, while the temperature on the distillate side of the membrane is maintained. After a specific sampling time, the hot feed stream is circulated into the distillate side of the membrane, effectively reversing the driving force across the membrane. Prior to either flow or temperature reversal implementation, the DCMD evaluation was stopped before scaling

occurred or after recovering 35-40% of the feed water. The results indicated the successful maintenance of water flux and salt rejection using both methods, with the temperature reversal method exhibiting better overall performance [121]. Both techniques effectively inhibited homogeneous salt precipitation and disrupted the nucleation of salt crystals on the membrane surface, leading to reduced fouling and improved membrane performance.

To prevent dye fouling in MD, the AGMD, SGMD, and VMD are commonly considered advantageous. In AGMD, there is an air gap between the membrane and the condensation surface. The feed solution is circulated on one side of the membrane, and cold air or an inert gas is passed on the other side to condense the vapour. The air gap acts as a physical barrier, preventing direct contact between the membrane and the condensation surface, thus reducing fouling. In this case, dye molecules are less likely to come in direct contact with the membrane surface, thereby minimizing fouling [122]. The SGMD involves the use of a continuous flow of a sweeping gas (e.g., air or nitrogen) on the permeate side of the membrane. The sweeping gas carries away the vapour molecules that pass through the membrane, preventing them from condensing on the permeate side and reducing the CP. This setup helps to maintain a clean and clear permeate side, minimizing the chances of dye molecules accumulation on the membrane surface [123]. The VMD is characterized by low-temperature differences due to negligible heat conduction, thus minimizing polarization and reduces fouling. However, the VMD is susceptible to wetting due to possible operating pressure exceeding the membrane LEP, thus compromising the separation efficiency.

3.2.3. Cleaning processes

Exploring the factors influencing membrane fouling is crucial to decrease the fouling rate and prolonging the membrane lifespan in the MD process. Nonetheless, it is practically impossible to

avoid fouling in the membrane processes. Thus, cleaning becomes important to remove foulants from the membranes. According to the reported findings, membrane cleaning mechanism is mainly categorised into pre-treatment, physical and chemical cleaning with the latter being more effective to remove the foulants and scalants deposited on the membrane [107]. Dow et al. (2017) evaluated effectiveness of foam fractionation as a pre-treatment method for textile effluent prior MD purification [124]. To produce the "fractionated MD feed," the textile effluent was treated through a foam fractionation. Afterwards, the pretreated feed was directed into the MD process for further treatment. Foam fractionation aims to remove surface-active agents, especially dye molecules from the feed stream by injecting it with compressed air. During foam fractionation, the feed water flowed down a column with an exposure to rising finely dispersed air bubbles. The gas bubbles effectively captured surface-active materials, lifting them to the top of the water column to form a foam layer. This foam layer was subsequently collected in a foam trap and removed from the system. According to the reported findings, the flux of the membrane module (effective surface area: 6.4 m^2) was only reduced from an initial rate of 5 to 2 $L \cdot m^{-2} \cdot h^{-1}$ after more than 1560-h of continuous operation without having membrane cleaning process.

In practice, chemical cleaning restores the membrane's initial performance to certain degree depending on the severity of fouling (**Figure 8**). Manzoor et al. (2022) investigated the impact of chemical cleaning using 2 wt% sodium hypochlorite (NaOCl) and 2 wt% citric acid in a novel hybrid MD combined with a submerged anaerobic membrane bioreactor to remove cibacron yellow, cibacron blue and methylene blue dyes [125]. The chemical cleaning procedure was implemented when the flux dropped to approximately 80% of the initial flux. To ensure optimal flux recovery, the module was detached from the MD system. The membrane was first washed with tap water to eliminate sludge layers and other impurities accumulated on its surface. Subsequently, chemical cleaning was carried out, involving a 15-min soaking of the membranes in NaOCl solution to remove organic foulants. This was followed by exposure to citric acid solution

618 to remove inorganic foulants. The chemical cleaning approach achieved 84.8% flux recovery
619 (**Figure 8a**).

620 According to Shi et al. (2022), a combined chemical cleaning approach, involving the use of
621 absolute ethanol and 0.1 $mol \cdot L^{-1}$ NaOH effectively maintain the permeate flux of VMD during
622 purification of CR dye [126]. The hollow fibre membrane demonstrated a remarkable dye rejection
623 ≥ 99%. However, the permeate flux gradually decreased from 18.2 [1] to 9.6 $kg \cdot m^{-2} \cdot h^{-1}$ after 8-h
624 operation. To minimize flux decline, a cleaning solution comprised of absolute ethanol and NaOH
625 was introduced as the feed solution and circulated through the fibre lumen using a diaphragm
626 pump under 0.1 MPa for 1 h. Subsequently, the membrane was further washed with pure water
627 for 30 min. The cleaning process gave rise to a remarkable 90% permeate flux recovery (**Figure**
628 **8b**).

629 To the best of our knowledge, physical cleaning methods are not widely studied in MD for dye
630 removal. This is mainly attributed to the nature of dye fouling in MD, which often involves the
631 adsorption and deposition of dye molecules on the membrane surface. These foulants exhibit a
632 strong affinity to the membrane material, leading to robust adhesion. As a result, physical cleaning
633 methods are not effective in removal of dye solutes from the membrane. Moreover, membranes
634 used in MD process typically have a small pore, making it challenging to physically access and
635 clean dye foulants from the membrane microstructure. Julian et al. (2018) evaluated air
636 backwashing to restore the flux of VMD membrane during desalination of the brine [127].
637 According to the research findings, magnesium deposition on the surface and pores of the
638 membrane, reducing flux upon increase in frequency and duration of backwashing. Magnesium
639 disposition was induced by nucleation causing salt crystallization. To some extent, air
640 backwashing reduced the membrane scaling. However, other physical methods such as aeration
641 and Vibration/ultrasound presented improved flux restoration of MD systems [128]. In aeration,
642 the air bubbles promote formation of the shear force which reduce the cake layer formation on

the membrane. In vibration processes, the cavitation is formed from small bubbles [128]. The collapse of these cavities generates shockwaves which detach the foulants from the membrane.

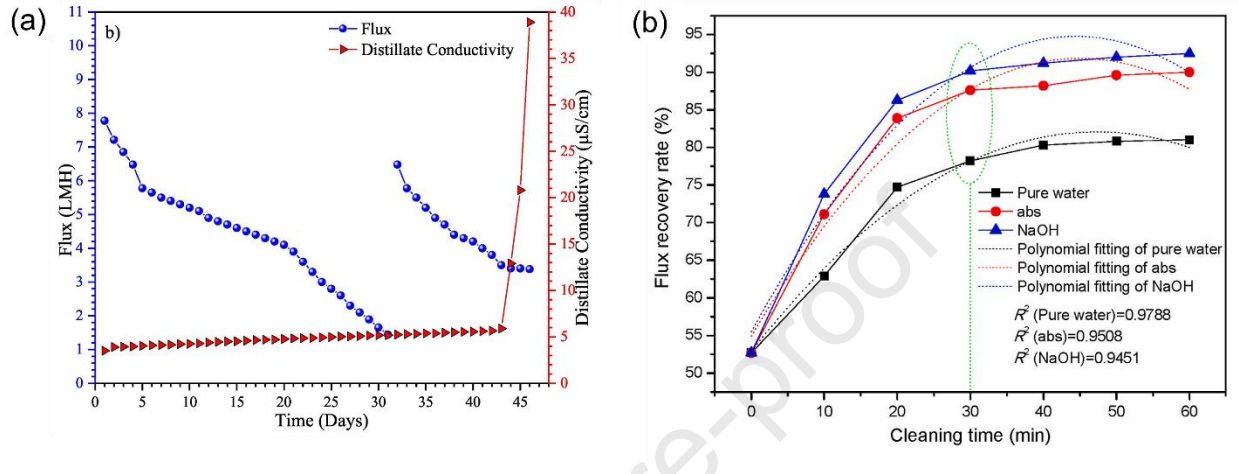

Figure 8. (a) Permeate flux and conductivity during 2 wt% NaOCl and 2 wt% citric acid chemical cleaning [125]. (b) Comparison of different chemical cleaning methods in retrieving the flux of membrane used for VMD process towards CR dye removal [126].

3.2.4. Hybrid/integrated MD processes

Treatment of dye wastewater through Integrated chemical and treatment processes has gained a remarkable research attention. Research has been focused on the hybridization of photocatalysis and membrane separation, also known as photocatalytic membrane reactors (PMR) [129]. However, coupling of MD with other membrane systems for the removal of dyes from wastewater has been evaluated extensively [130,131]. Ge et al. (2012) used a polyelectrolyte-promoted forward osmosis-membrane distillation (FO-MD) hybrid system to recycle acid dye-containing wastewater [131]. MD was used to reconcentrate the poly(acrylic acid) sodium (PAA-Na) salt used as the solute in the FO process to dehydrate the wastewater.

Based on reported findings, FO-MD hybrid process is more efficient than the individual FO process in concentrating acid orange 8 dye present in the wastewater. As suggested by the authors, integration of FO and MD combines the strength of both processes, including low fouling tendency and the potential use of industrial waste heat [131].

The FO-MD hybrid process can potentially achieve zero liquid discharge when treating wastewater from the textile industry and recover valuable dye molecules while producing high-quality water. However, efficient FO and MD membranes are required to reduce fouling and advance this hybrid process [132]. Li et al. (2020) identified an internal concentration polarization (ICP) effect and membrane fouling using two commercial FO membranes, which make it difficult to equilibrate the water transfer rate to reach good performance [132]. Also, the authors proposed a hybrid FO-MD system composed of an asymmetric membrane and PTFE membrane in the FO and MD units, respectively [132]. During the test experiments, the draw solution was diluted in the FO process and was simultaneously regenerated in the MD process. The system was able to treat textile wastewater in continuous and stable operation due to the fouling and ICP resistance of the FO symmetric membrane. Also, the use of the symmetric membrane reduced the energy consumption, and the overall cost of a large-scale RO-MD system.

More recently, a FO-MD hybrid process using a newly developed graphene oxide enhanced FO membrane (GFO) was proposed to treat textile wastewater. Wu et al. (2024) used textile wastewater to evaluate the GFO performance [133]. The feed matrix presented a significant challenge on membrane performance and stability due to a higher degree of fouling and wetting [118]. The GFO membrane was fabricated through interfacial polymerization process by adding GO into the polyamide. The performance of the hybrid system with GFO membrane was compared to the performance of a commercial FO membrane. According to the reported findings, GFO-based FO-MD process presented improved fouling resistance and stable permeate flux. The

hybrid system surpassed the individual FO and MD processes by overcoming the limitations of FO draw solution dilution and MD membrane wetting challenges [133].

A MD/photocatalysis hybrid process has been studied to treat dye wastewater due to the ability to retain non-volatile compounds [134]. The quality of the permeate in MD/photocatalysis hybrid process is not affected by the presence of the catalyst at concentrations range of 0.1-0.5 $g \cdot L^{-1}$ However, concentrations higher than 0.5 $g \cdot L^{-1}$ promote formation of a catalyst cake layer on the membrane surface, thus reducing permeate flux [134]. The catalyst characteristic, including the crystalline phase and particle size plays an important role in controlling fouling of the MD/photocatalysis hybrid process during of dye-polluted wastewater. According to Mozia et al. (2008), P25 (TiO_2 in anatase and rutile phase) showed the best performance due to high purity anatase-phase TiO_2 structure [135].

4. Energy consumption and module design

Thermal energy consumption is a critical factor in economic viability and environmental sustainability of any separation process, including MD. In fact, the high energy consumption of MD has been identified as one of the major limitations of the process and different efforts have been devoted to reducing the required thermal energy of the process. The energy consumption and gain output ratio (GOR) of various MD configurations are presented in **Table 3**.

Table 3: The comparison of energy consumption and GOR for various MD configurations.

MD configuration	**Feed and permeate temp. (°C)**	**Permeate flux ($kg \cdot m^{-2} \cdot h^{-1}$)**	**Energy consumption (kWh/m^3)**	**GOR**	**Ref.**

and feed solution					
DCMD, 3.0% NaCl	41 and 26	6.0	780	0.86	[136]
AGMD, seawater	64.0 and 20	3.3	605	0.73	[137]
AGMD, seawater	70 and 25	13.0	1080	0.43	[138]
AGMD, 3.5% NaCl	70 and 25	1.0	105	6.5	[139]
DCMD, seawater	85 and 20	2.1	200	6.0	[140]
DCMD, seawater	-	2.5	302	0.9	[141]
AGMD, seawater	85 and 30	3.4	210	-	[142]
DCMD	80 and 20	1.9	205	5.8	[143]

The main strategies used to reduce the thermal energy requirements of MD include process optimization and utilization of waste thermal energy in the textile industry, innovative module designs and configurations, and fabrication of new membranes with low-thermal losses. On the process end, several parameters including feed and permeate temperatures, feed and permeate flow rates, and properties of the feed solution affect the thermal energy consumption of the process [144,145].

(a) Effect of feed temperature

Flux in MD is exponentially linked with the temperature of the feed solutions whereas the heat conduction through the membrane is linearly related to the temperature difference between the feed and permeate sides [146,147]. Therefore, the thermal efficiency of the process, measured as the ratio of convective heat transport to the total heat transport across the membrane, increases with an increase in feed temperatures. However, for poorly insulated systems, high feed temperatures deteriorate the system performance due to the high losses of heat from the feed stream to the environment. According to Elmarghany et al. (2019), the feed temperature presents the adverse impact on thermal efficiency, primarily attributed to heat dissipation from the membrane cell into the surroundings [148]. The rise in feed temperature resulted in a greater temperature disparity between the cell and its surroundings, causing a 34% reduction in thermal efficiency. Additionally, the obtained output ratio declined from 0.96 to 0.6, accompanied by a rise in specific energy consumption from 689 to 1037 $kWh \cdot m^{-3}$.

In the case of DCMD, the system performance is dominantly dependent on the feed temperature and the effect of permeate temperature remains relatively minor. For instance, Song et al. (2007) performed a systematic investigation of the effect of feed and permeate temperatures using a commercial hollow fibre membrane module [149]. Reportedly, the increase in feed temperature from 40 °C to 92 °C led to an exponential increase in permeate flux whereas increasing distillate temperature from 32 °C to 60 °C did not influence the flux notably. Shirazi et al. (2020) utilized the waste thermal heat to generate > 60 °C for use in pilot scale MD treatment of textile wastewater [52]. The experiment was conducted during cold season (environmental temperature of 1-5 °C), thus indicating the possible opportunity to reduce the external energy requirement for treating textile wastewater on a large scale. The unique properties of the membrane improved the process

735 performance where a permeate flux and salt rejection of 28.31 $kg \cdot m^{-2} \cdot h^{-1}$ and 98.15% were
736 recorded respectively compared to the commercial membrane (flux: 18.50 $kg \cdot m^{-2} \cdot h^{-1}$ and salt
737 rejection: 97.10%), without considerable pore wetting. Also, it was reportedly indicated that new
738 membrane possessed lower LEP owing to its higher porosity, larger maximum pore size (0.76
739 µm), and thinner structure (150 µm).

740

741 (b) Effect of feed flow rate

742 Feed flow rate is another important parameter influencing the energy consumption of the MD
743 process [150,151]. The temperature polarization (TP) (which refers to a discrepancy between the
744 temperature of the bulk feed solution and the temperature at the interface of the membrane)
745 remains a significant challenge hindering the thermal efficiency and mass transfer coefficients of
746 the MD process. The feed flow rate affects the residence time of the solution in the membrane
747 module. The flow rate of the hot feed affects the heat transfer efficiency across the membrane.
748 Higher flow rates induce better mixing of the fluid present at the membrane surface and in the
749 channel leading to reduced TP. This results in higher driving force (temperature differences) to
750 the vapour transport from the feed to the permeate side. Also, a high flow rate decreases the
751 residence time of the feed solution in the membrane module resulting in a high average
752 temperature over the membrane length [152]. Moreover, higher feed flow rates delay the
753 membrane fouling. This can be more important in case of textile wastewater treatment, as
754 different types of dyes, chemicals, and inorganic compounds are present in the solution [153].

755 Although the positive impact of high flow rate on the energy efficiency of MD process is well
756 documented, it should be noted that beyond a threshold level, further increase in flow rate
757 influences the process performance negatively. According to Duong et al. (2016) running the pilot-
758 scale AGMD process with a high-water circulation rate led to a decrease in thermal efficiency

[139]. When the water circulation rate was increased, the time the coolant and hot feed spent inside the membrane module decreased, causing a reduction in the effectiveness of heat recovery. Technically, the recovery of latent heat from water vapour to the coolant diminished, causing an increase in temperature difference between the evaporator inlet and the condenser outlet. The higher water circulation rate increased temperature difference between the evaporator inlet and the condenser outlet, contributing to a rise in the overall heat input to the system. This increase in total heat input occurred at a faster stride compared to the rate of distillate production when the water circulation rate was elevated. Consequently, the specific thermal energy consumption of the system increased from 65 [3] to 105 $kWh \cdot m^{-3}$ as the water circulation rate was raised from 150 to 350 $L \cdot h^{-1}$. Also, this shift caused the GOR of the system to decrease from 9.5 to 6.0. Similar effects of water circulation rate on thermal efficiency were reported in other studies [154,155]. According to the research findings, water circulation rate had a significant impact on the specific electric energy consumption of the system. This was directly related to the water circulation rate and the hydraulic pressure drop across the membrane module. When the water circulation rate was increased from 150 to 350 $L \cdot h^{-1}$, the hydraulic pressure drop increased from 0.14 bar to 0.45 bar. Despite the increase in distillate production rate, the specific electric energy consumption of the system showed a notable increase from 0.1 to 0.4 $kWh \cdot m^{-3}$.

In MD, water vapour mass transfer through the membrane is essential. When the flow rate is too high, the process performance remains relatively constant due to the shift of mass transport limit from the flow channels to the membrane [156,157]. As a result, thermal efficiency of the process decreases, necessitating higher temperatures and subsequently increasing energy consumption. Flow rates influence the pressure drop across the membrane module. Excessively high flow rates elevate pressure drop, leading to increased pumping energy requirements. Balancing flow rates to minimize pressure drop while maintaining sufficient mass transfer is crucial for optimizing energy consumption. Extremely high flow rates increase the risk of membrane wetting, where the

784 hydrophobic membrane becomes wetted by the liquid feed leading to reduced vapour flux and
785 poor permeate quality [158]. Technically, the pumping pressure should be maintained below the
786 LEP of the membrane.

787

788 (c) Effect of module spacers

789 To overcome the negative impacts associated with the high flow rate in the MD system, various
790 options have been proposed to alleviate the TP and CP. Among other strategies, spacers are
791 used in flat sheet membrane modules [159–161]. The spacers (net-like feed channels) enhance
792 performance of MD systems. These spacers, with various designs and orientations, are reported
793 to reduce thermal polarization effects and improve permeate flux [160,162]. Their introduction
794 leads to a decrease in the temperature differences across the membrane and effectively
795 increases mass transfer rates. However, the increase in spacer void beyond 60% optimal range
796 negatively impact mass flux [162]. Despite some pressure drops caused by spacer channels, their
797 benefits in reducing thermal boundary layers and CP are reported [163,164]. Achieving optimal
798 conditions for spacer installation in a DCMD system is crucial for maximizing mass transfer
799 efficiency and minimizing heat transfer effects depending on various parameters.

800

801 (d) Effect of module design

802 In addition to spacers, another strategy capable of decreasing the thermal energy requirement of
803 MD is the design of energy-efficient MD modules. A module fundamentally provides housing to
804 accommodate the membranes. However, a more favorable design revolves around embracing a
805 module configuration to boasts superior hydrodynamic conditions on both shell and lumen sides
806 [165]. Depending upon the configurations of membrane (flat sheet or hollow fibre) and MD

807 (DCMD, AGMD, VMD, and SGMD), several module designs to improve heat and mass transport
808 of MD process have been proposed [166–168].

809 Notable flat sheet membranes designs include spiral wound modules, muti effect VMD modules,
810 and "gap" MD modules. The latter category mainly involves the module designs built for the
811 AGMD where a gap between the feed and condensing surface is provided. Traditionally, the gap
812 is filled with a thin film of air giving rise to AGMD. However, recent studies use various materials
813 including water, conductive metals and sand to fill the gap, thus giving rise to material gap
814 membrane distillation (MGMD) [169–172]. The inclusion of these materials in the gap improves
815 the heat transport from the condensing surface and therefore, yields high flux and lower specific
816 thermal energy consumption. Similar to the flat sheet membrane modules, innovative module
817 designs have been proposed for hollow fibre MD modules. The main innovative aspect of these
818 modules is the shapes of the fibre where helical, wavy, curly, and spacers knitted fibres have
819 been proposed to improve the thermal efficiency of the MD process [166,173]. Notably, most of
820 these studies considered the desalination application of various MD configurations, while few
821 studies on module design have been specifically developed for MD-based textile wastewater
822 treatment. Nevertheless, most of the investigated scenarios in MD module design can be
823 considered for this application as well, either directly or with some minor modifications according
824 to the nature of effluent from textile industry.

825 In addition to the new designs of module housing and fibre shapes, the design of optimum contact
826 length (or effective module length) has also been an important parameter to reduce the thermal
827 energy requirement of MD process. Theoretically, greater contact lengths can be achieved by
828 elongating the membrane (or fibre length in hollow fibre setups). However, practical difficulties
829 involving technology, handling, and installation render the preparation and use of very long
830 modules unfeasible. As an alternative, achieving a substantial contact length involves either
831 connecting numerous modules in a series or increasing the membrane length within each section

of a flat sheet membrane. In the context of spiral-wound flat sheet membranes, extending the flow channel length from 1 to 7 m increases the GOR by 3-fold [174]. Similar findings were reported by Winter et al. (2017) where specific thermal energy consumption of MD was reduced from 296 to 107 $kWh \cdot m^{-3}$ after increasing the channel length from 1.5 m to 5 m [174]. However, in case of textile wastewater treatment, the spiral wound module is highly susceptible to fouling due to high contamination level of dyeing wastewater and its inorganic content. Separately, Ali et al. (2018) reduced the specific energy consumption of DCMD by over 20% after increasing the channel length (with an effect comparable to elongating the module length) from 1 m to 10 m [147]. Similar findings were reported in another investigation where channel length elongation from 3.5 m to 10 m reduced the specific energy consumption of AGMD by 46% [175].

(e) Effect of membrane properties

Membrane properties play a significant role in dictating the energy consumption of the process. Membrane properties including thickness, porosity, tortuosity, and pore size play a crucial role in influencing permeate flux, heat, and mass transfer coefficients. Thinner membranes offer higher mass transfer and flux. Due to the small thickness, the mass transfer resistance is significantly reduced, ensuring high permeate flux. However, this phenomenon establishes a trade-off between heat and mass transfer. Although thinner membranes enhance heat transfer, they cause performance decline. The increased heat transfer increases TP, thus reducing the vapour pressure gradient and therefore the flux. Balancing these properties is key in membrane design.

Based on previous research findings, energy-efficient membranes should have thicknesses between 20 and 60 μm, pore diameters of 0.3 μm for high LEP, porosity above 75%, and specific mechanical strength [145]. According to theoretical and experimental reports, small membrane thickness reduces the thermal efficiency of materials like PVDF and PTFE. For a heat transfer

856 coefficient of 600 $W \cdot m^{-2} K$, membrane thickness in the range of 150–200 μm is considered optimal
857 to achieve 80% efficiency in a DCMD system [176]. Therefore, thicker membranes are high
858 energy efficiency during MD treatment of high saline feed water. However, for low solute
859 concentration range, such as diluted textile effluent, thinner membranes can provide higher
860 permeate flux and energy efficiency [177]. The development of multilayer membranes emerges
861 another promising approach to address energy efficiency. In this design, a strategically placed
862 insulating layer is situated as the intermediate layer inside the membrane structure. The presence
863 of an insulating layer serves as a thermal barrier, effectively mitigating the transfer of heat by
864 conduction across the membrane, specifically in the DCMD configurations. Afsari et al. (2023)
865 used this approach to develop a novel nanofibre membrane with enhanced total thermal efficiency
866 [178]. The authors focused on the development of a triple-layer membrane featuring a nanofibrous
867 structure for processing high salinity water using DCMD. According to the obtained results, the
868 triple-layer membrane structure reduced the energy consumption by 20% in comparison with the
869 traditional single-layer membrane structure.

870

871 **5. Heat and mass transfer modelling**

872 Mathematical models and numerical designs have been reported in the literature to simulate the
873 flux of VMD configuration [179]. These models could be adapted to other MD configurations,
874 including AGMD and SGMD. These models include one-dimensional (1D), two dimensional, and
875 three dimensional (3D) approaches [179–181]. The 1D models have been used to determine the
876 role of process variables on the MD performance. However, the models are unable to provide
877 information about the module and membrane geometry, which is critical to scale up the process.
878 The 2D models have been used to analyze the permeation rate and heat and mass transfer effect
879 on the MD process. This type of model has limitations in evaluating the membrane characteristics

and composition along with the geometry of the module [179]. In contrast, the 3D models provide a detailed visualization of the processes occurring inside of the membrane, including the impact of boundary layers and the polarization effects related to the characteristic of the membrane, such as porosity and tortuosity [179]. Various case studies evaluating mathematical models and numerical designs are comprehensively elaborated below.

A 3D computational fluid dynamics (CFD) model was evaluated by Baghel et el. (2020) using COMSOL Multiphysics to model the interfacial temperatures for Naphthol Blue-Black dye from wastewater and predict the flux in VMD [179]. The CFD model incorporated the transport equations for momentum, heat, and mass transfer. The heat and mass transfer were coupled at the contacting interfacial boundaries between the feed solution and the membrane surface, and the effect of variables such as flow and temperature. Also, the amount of vacuum and concentration on the permeate flux were analysed [94]. Similarly, a theoretical permeate flux was evaluated from the convective heat transfer through the porous membrane. The model combined the Knudsen and Poiseuille flow equations to study the vapour transport through the porous membrane [179,182]. The model fitted well with experimental data and provided the temperature polarization coefficient (TPC) for the VMD process at different operating parameters. Based on the model, the feed temperature and vacuum degree were the main parameters affecting the permeate flux and minimum specific energy consumption. Also, increasing the feed temperature from 25 °C to 85 °C reduced the TPC from 0.81 to 0.48, which was reflected in a reduced heat transfer resistance and a considerably increase of the permeate flux [179].

Figure 9a shows the temperature contour and convective heat flux inside the membrane of the VMD module at 85 °C as obtained by the CFD model. According to the reported findings, driving force of the process, represented by the difference in transmembrane vapour that increases

904 exponentially when the feed temperature increases, caused this temperature profile [179]. The
905 accumulation of dye on the feed side of the membrane during the transport of water vapour
906 through the membrane, caused a resistance to liquid-mass transfer, and therefore reduced the
907 passage of water vapour. The small pore size and hydrophobic properties of the membrane
908 contributed to the accumulation of the dye on the membrane surface. The CP effect on the feed
909 side of the membrane become significant due to the increased accumulation of dye at the
910 membrane surface. Notably, the performance of the VMD process can be improved by removing
911 the dye from the surface of the membrane with distilled water. After 60 h of running and washing
912 the membrane, a 99.9% removal of dye with a permeate flux of 44.94 $kg \cdot m^{-2} \cdot h^{-1}$ was obtained,
913 thus presenting 99% flux recovery.

914

915 A 3D CFD model was developed to study the thermal velocity and concentration field of a VMD
916 using PFTE membranes to treat methyl orange dye wastewater. Initially, the optimal operating
917 parameters of VMD, including mass flow rate, vacuum pressure, inlet feed temperature, and dye
918 concentration, were optimized using response surface methodology (RSM) [183]. A regression
919 model was developed to describe the permeate flux, dye rejection, and specific energy
920 consumption (SEC). The 3D CFM model was applied to the optimized parameter conditions
921 (permeate flux of 19.60 $L \cdot m^{-2} \cdot h^{-1}$, dye rejection of 99.80%, and SEC of 2.04 $kWh \cdot m^{3}$) to obtain the
922 permeate flux profile and dye rejection of various cycles of VMD operation with intermittent
923 washing and to understand the fouling behaviour of the membrane. The model captured the
924 evaporation in the feed at the membrane surface and the condensation of vapours in the permeate
925 at the membrane surface. **Figures 9b-d** show the thermal field, velocity field, and concentration
926 field in the membrane module obtained from the 3D CFD of the RSM optimized input process
927 parameters. After conducting SEM analysis of the PTFE membranes, the dye deposition was not
928 severe due to high hydrophobicity, LEP, and pore wetting resistance of the membrane. The

membranes exposed to long-term VMD operation didn't show any significant alterations, showing that the PTFE membrane could retain the initial structure and property during dye treatment [183].

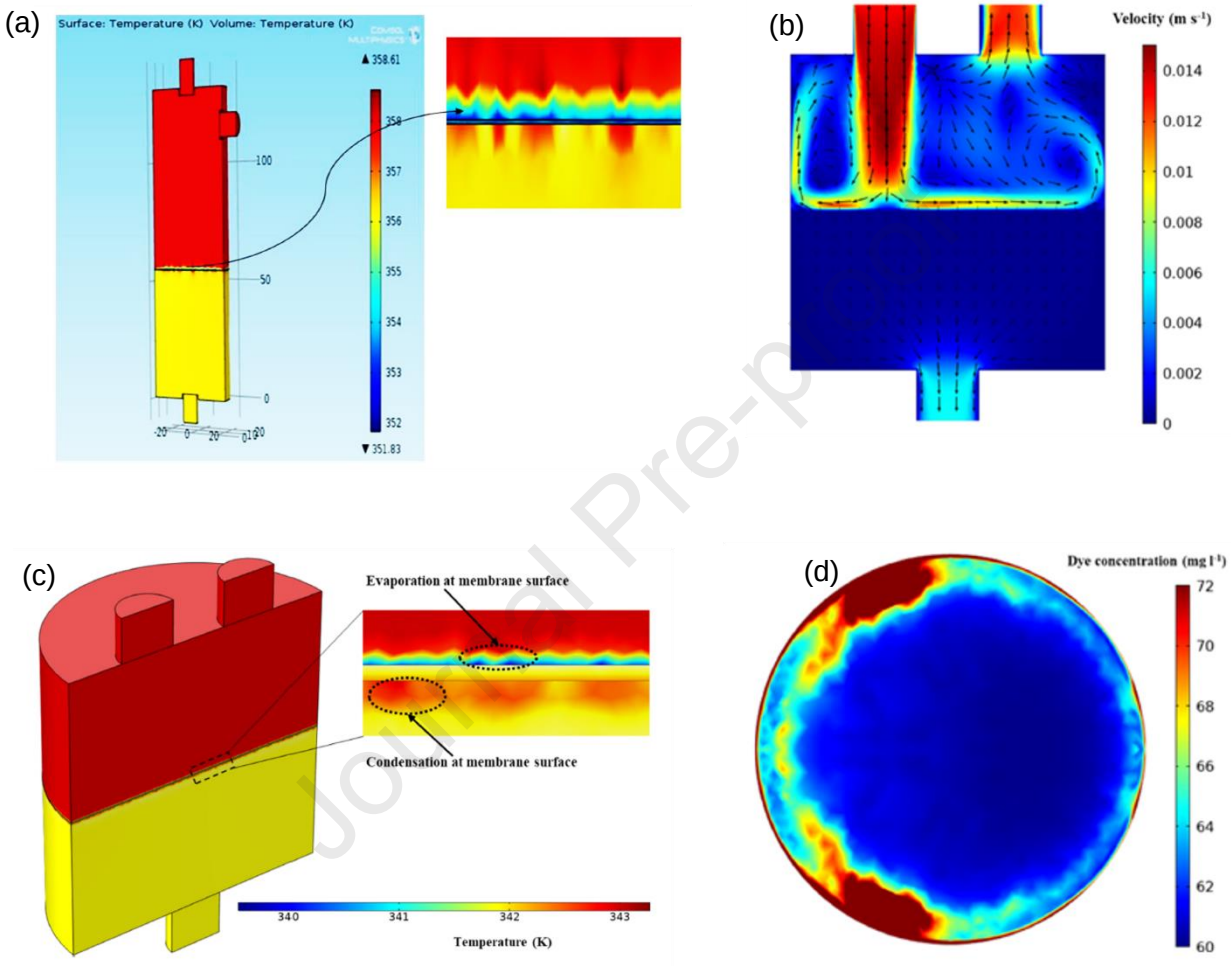

Figure 9. (a) Temperature contour inside a VMD module at 85 °C feed temperature, Naphthol Blue-Black dye concentration of 300 ppm as simulated by CFD using COMSOL Multiphysics software. Operating conditions: flow rate of 5 L·min^{-1}, vacuum of 750 mmHg [179], (b) velocity field, (c) thermal field, and (d) concentration field in the membrane module obtained using 3D CFD at optimized input process parameters from RSM [183].

A mathematical model incorporating temperature and CP effects was developed by Banat et al. (2005) to treat MB dye solutions generated by the textile industry using VMD [184]. The model was validated with experimental data. The model incorporated heat and mass transfer principles, including 1) flux in the boundary layer to the membrane surface, 2) evaporation at the pore entrance and diffusion of the vapour through the pore, and 3) diffusion of the vapour beyond the pore and recovery. The model was validated by comparing the predicted variation of MB concentration with time to the experimental data. The experimental data was comparable with the model predictions. The permeate flux rate decreased exponentially with time, and the dye was concentrated in the feed reservoir without detection in the permeate. The permeate flux was strongly dependent on feed temperature but was independent of salt concentration [184].

As the filtration effectiveness depends on the membrane characteristics, recent studies show the potential of surface modification with carbon-based materials like GO and CNT. GO as 2D material can enhance the operation yield and protect against fouling for its negative charge onto a surface behaving as polyanion. Hence, GO can interact electrostatically with positively charged molecules and materials present in the wastewater enabling electrostatic repulsion of negatively charged molecules like anionic dyes [185,186]. Besides 2D materials like GO, other types of nanomaterials that are based on carbon are 1D CNT including single (SWCNT) and multi-walled nanotubes (MWCNT). They are added to reduce the wettability of the membrane for their hydrophobic properties [187]. Moreover, their high surface area and porosity improves absorption of the pollutants in selected wastewater treatment applications. Membranes modified with CNT offer enhanced mechanical stability, self-cleaning functions, and anti-fouling capacity of the

962 nanocomposite membrane [188]. The immobility of the CNT into the membrane surface occurs
963 due to charge, van der Waals interactions, and chemical bonding [189].

964 To improve the hydrophobicity of the membranes, the ZIF NPs can also be added. Tournis et al.
965 (2022) proposed the use of ZIF NPs to modify the porous PVDF–HFP membranes. Membrane
966 modification significantly reduced the wettability of the membrane [190]. Another group of filler
967 membrane materials is ZIF. A series of DCMD experiments in combination with numerical
968 modelling using JAVA software were conducted to study the water flux and rejection rate of
969 simulated solutions containing salts and dyes and the mass transfer behaviour of the MD process.
970 A composite ZIF doped in PVDF-co-HFP nanofibrous membrane synthesized by the
971 electrospinning technique was used. The salts and dye solutions were prepared by mixing acid
972 red, acid yellow, methylene blue, and crystal violet with NaCl. The ZIF/PVDF-co-HFP membrane
973 showed high permeate flux (19.2 $L \cdot m^{-2} \cdot h^{-1}$) and a dye rejection ≥ 99.99% compared to the pristine
974 PVDF-co-HFP membrane and a commercial PVDF membrane. To model the DCMD process, the
975 membrane was orderly divided into N different blocks per 1 cm. The TPC of different nanofibres
976 was theoretically calculated by determining the saturated and unsaturated vapour pressure of
977 the first membrane block using the Antoine equation and a partial pressure equation of non-ideal
978 binary mixtures [191,192]. Also, by calculating the membrane water permeation by iteration, the
979 water permeation coefficient of different ZIF/PVDF-co-HFP membranes was obtained. The water
980 flux was simulated by dividing the membrane into 30 blocks, each with a length of 1 mm, and by
981 calculating the flux in every block. The model showed good accuracy with respect to the
982 experimental and simulated water flux. The negatively charged acid red and acid yellow dyes
983 were effectively rejected compared to the methylene blue and crystal violet dyes due to the
984 negative charge characteristics of the ZIF/PVDF-co-HFP nanofibrous membrane [191].

985

Textile industries release high temperature wastewater that can potentially be treated by MD processes. In this process, the heat already present in the discharge solution is used to provide the energy for MD processes [193]. However, one of the main limitations of industrial wastewater is the presence of organic compounds, softeners and levelling agents, such as surfactants, which can cause fouling or wetting of the membrane. The presence of surfactants reduce the surface tension and thus, the LEP of the membrane and impact the MD performance [194]. An agarose hydrogel thin layer attached to the surface of a hydrophobic porous PTFE membrane was used to investigate the impact of hydrogel properties on the membrane wetting during the MD treatment of polyester fabric dyeing wastewater exposed to different types of surfactants. The agarose is a linear polymer with a molecular weight of 120 kDa [195]. According to the reported findings, the unmodified MD membrane decreased flux rapidly, and the conductivity increased in a short period of time, indicating the occurrence of membrane wetting due to the presence of the surfactant. However, with the PTFE-agarose treated membrane, the flux and the conductivity remained unchanged for 24 h. The agarose layer repelled the hydrophobic moiety of the surfactant, which in turn prevented the formation of micelle; therefore, preventing the surfactant from penetrating through the hydrogel layer to cause membrane wetting [195]. Furthermore, the flux of the MD process using the PTFE-agarose treated membrane is not limited by mass transfer through the hydrogel [195]. The flux variation was attributed to the lower heat transfer coefficient of the protective layer, which reduces the vaporization temperature, causing flux decline while improving membrane resistance to wetting. Increasing the surface area of the membrane or the thermal conductivity of the protective hydrogen layer, the MD efficiency for dyeing wastewater treatment remain the same [195,196]. **Figure 10** shows the temperature profile of the PTFE-agarose protected membrane, the rejection of the hydrophobic moiety of the surfactant by the hydrogen protective layer, and the penetration of surfactant micelles through the hydrogen layer during the MD process, respectively.

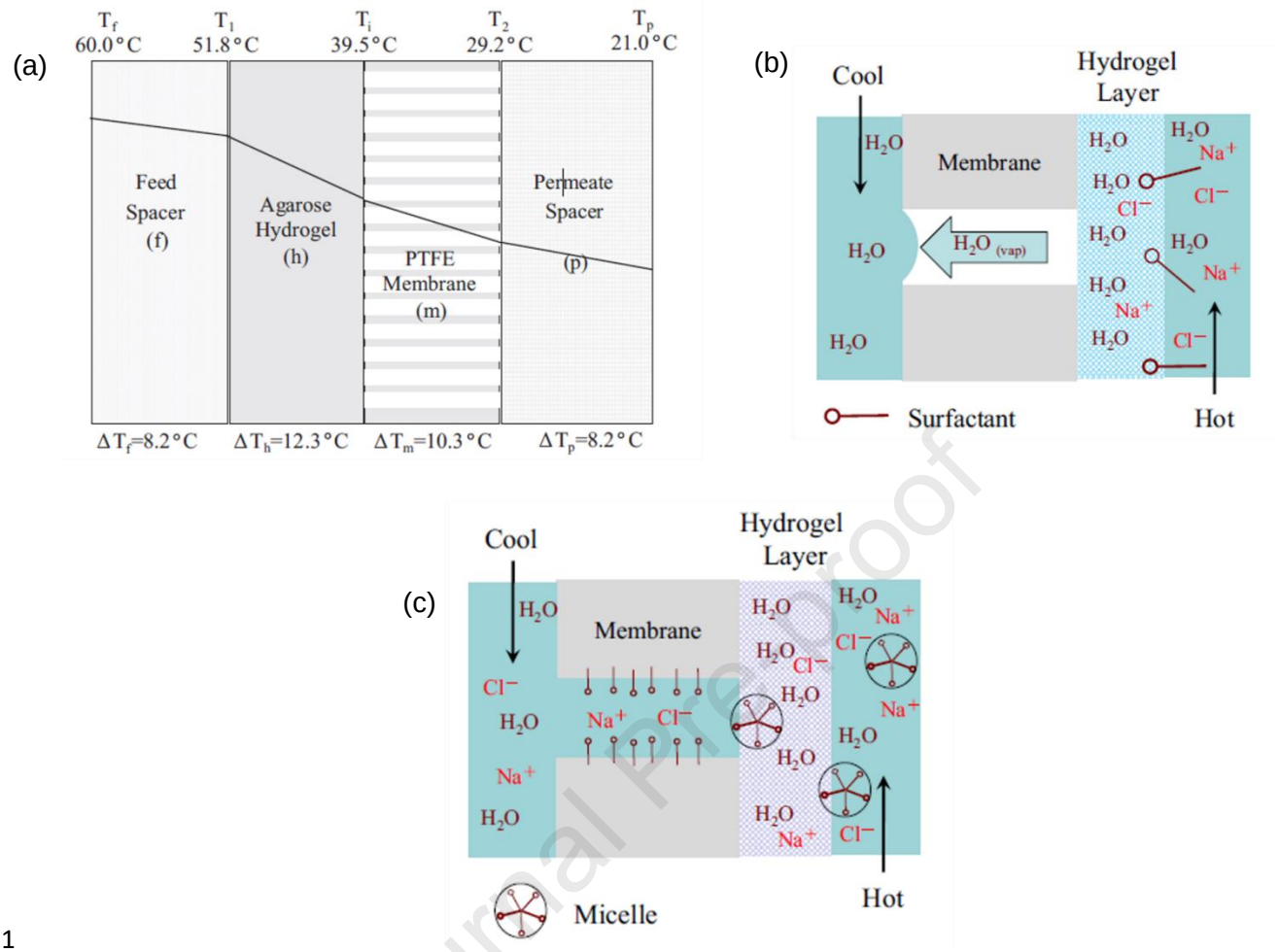

1011

1012 **Figure 10**. (a) temperature profile of the PTFE- agarose protected membrane. The mechanism
1013 for (b) the rejection of the hydrophobic moiety of the surfactant by the hydrogen protective layer
1014 and (c) penetration of surfactant micelles through the hydrogen layer during the MD process [195].

1015

1016 The micelle formation was explained by Musnicky et al. (2011) by conducting studies on the
1017 gradient diffusion of surfactants such as ionic sodium dodecyl sulfate (SDS) micelles in agarose
1018 gel, and by comparing the results with published theories [197]. The study used holographic
1019 interferometry to measure the gradient diffusion coefficient at different sodium chloride, gel, and
1020 surfactant concentrations. Based on the reported findings, micelle diffusivity increased linearly

with surfactant concentration with decreasing sodium chloride and gel concentrations. This behaviour suggested decreasing micelle-micelle electrostatic interactions with increasing sodium chloride concentrations. The concentration effect is quite strong for charged solutes, thus doubling micelle diffusion coefficient relative to its value in the same gel at infinite dilution. The study compared the extrapolated, infinite-dilution diffusion coefficients and the rate at which the micelle diffusivity increased with surfactant concentration with predictions of previously published theories in which the micelles are treated as charged, colloidal spheres and the gel as a Brinkman medium. The experimental data and theoretical predictions were in good agreement [197].

In a research study, micellar enhanced ultrafiltration (MEUF) integrated with VMD was used to remove methylene blue from aqueous solutions and treat the MEUF reject to increase water recovery [94]. A theoretical model based on modified resistances in series was used to determine the effect of feed dye concentration, surfactant concentration, and feed pressure on the flux of the MEUF process. The CFD model was used to predict the LEP of the VMD membranes in the presence of the dye. Sodium dodecyl sulphate and sodium chloride were added to the dye solutions as anionic surfactant and electrolyte, respectively, to promote micelle formation. A polyethersulfone (PES) membrane loaded with activated carbon was used in the UF process, and a tetraethyl orthosilicate crosslinked polysulfone (PS) membrane was used in the VMD process to treat the UF retentate. The resistance in series model predicted the operating parameters and generate a minimum error between predicted and simulated UF fluxes. The computational model provided an insight into the movement of fluid-fluid interface inside the pores of the membrane. The MEUF-VMD integrated system provided pure water while the two membranes remained stable. The system can operate in continuous mode by increasing the surface area of the VMD membrane to match the MEFU flux. The hybrid system could treat wastewater generated by the distillery, starch, pharmaceutical, and tannery industry [94].

6. Application of Machine Learning and Artificial intelligence in MD

Optimizing the MD process towards removal of dyes from water is experimentally time-consuming and expensive requiring the selection of many parameters [198,199]. The application of methods shortening process time, increase efficiency, and reduce the cost of the process is key. One of the most promising approaches involves the use of AI to model and optimize dye pollution removal [200–202]. The term AI covers many types of algorithms. Recently, attempts have been made to apply some algorithms to predict the optimal course of the water treatment process. Although AI has been evaluated in various treatment processes towards removal of dyes from wastewater, it is rarely reported in MD. Therefore, the AI-assisted MD in water treatment processes is recommended.

The most commonly applied in environmental sciences and biotechnology challenges are the classical neural networks, namely artificial neuron networks (ANNs) [203]. They are based on the model of a perceptron neuron known as the binary linear classifier [204]. In general, neural networks are the computational tools enabling computers to learn some patterns by analysing training datasets. In the case of the perceptron the input data enter the neuron model with appropriately assigned weights, they are summed up (i.e., they form the so-called weighted sum) and after applying the activation function (also known as step function) return the desired result. ANNs were used to predict the removal efficiency of the methylene blue [205]. The neural network consisting of ten hidden layers was applied [206]. The feedforward backpropagation algorithm was used for the classification tasks [207]. The proposed approach can be successfully applied to maximize the methylene blue removal with nano zero-valent aluminum (nZVAI). The ANNs with one hidden layer consisting of ten perceptrons (created with MATLAB 2019b packed software) were applied to the prediction of the CR adsorption [208]. Notably, AI-based algorithms have the

potential to be used as a supporting tool in the planning and development of more efficient dye removal.

Another AI-based algorithm applied in the dye removal process is Support Vector Machines (SVM). It is the concept of decision space, i.e., multidimensional hyperplane space separating cases belonging to different classes. The decision space is divided by building boundaries separating objects included in different [209]. The SVM-based algorithm predicts the methylene blue removal rate with high accuracy, and was therefore applied to the optimize the congo red adsorption [210]. The comparison of the AI-based algorithmic performance in the field of dye removal considering algorithms type, their application field, accuracy, the proportions of training sets, and inputs and outputs parameters is summarised in **Table 4**. Interestingly, AI-based algorithms are noteworthy computational tools in the context of predicting important parameters of the pollution removal process.

1082 **Table 4.** The comparison of the AI-based algorithms applied in dye removal.

Application field	***AI-based algorithm type***	***Accuracy***	***Training/ testing/validation sets [%]***	***Inputs parameters***	***Outputs parameters***	***Ref.***
Prediction of the MB removal efficiency	ANNs	0.97	60.00/20.00/20.00	11 experimental factors (residence time, initial MB concentration, temperature, pH, stirring rate, nZVI dosage, the concentration of two detergents: Ariel and Vanish, and the concentration of three salts: NaCl, Na_2CO_3, and Na_2SO_4)	MB removal efficiency	[205]
Prediction of the alizarin red S removal efficiency	ANNs	0.99	lack of information	4 parameters (pH, the initial Alizarin concentration in the feed, the extractant volume percentage in the organic phase, and the fluid flow rate)	Alizarin red S removal efficiency	[211]
Prediction of the CR adsorption	ANNs	0.99	lack of information	4 parameters (starting concentration, pH, temperature, time)	adsorp-	[208]

					tion capacity of CR	
Prediction of the malachite green	ANNs	0.99	lack of information	10 parameters (catalyst type, reaction time, light intensity, initial concentration, catalyst loading, solution pH, humic acid concentration, anions, surface area, and pore volume of various photocatalysts)	Malachite green degradation efficiency	[212]
Prediction of the CR adsorption	SVM	0.99	lack of information	4 parameters (starting concentration, pH, temperature, time)	adsorp-tion capacity of CR	[208]
Prediction of the MB degradations efficiency	SVM	0.94	85.00/15.00/0.00	4 parameters (pH, dye concentration, photocatalyst dose and irradiation exposure time)	MB removal rate (%)	[210]

1083 MB: methylene blue, ANNs: artificial neuron networks, SVM: Support vector machine

7. Challenges and prospects, and perspectives

Utilization of MD in treating the dye wastewater offers various benefits such as high removal efficiency and the process versatility in handling a wide range of dyes in various compositions. Also, MD is particularly effective in treating dye-contaminated waters under high salinity and elevated temperatures. During the process treatment, high-quality water is produced. Among other things, it provides a promising sustainable solution towards treatment of dye-contaminated wastewater due to low energy requirements. Also, advancements in membrane materials and optimization of the process performance and scalability pave a way to wide adoption of this process towards future dye-wastewater treatment. However, to ensure full adoption at industrial scale, various challenges including membrane wetting, fouling and requirement of high capital costs must be overcome. Also, system design with improved efficiency is imperative to minimize the process operating costs while promoting the attractiveness of the technology to dye wastewater treatment.

There are many challenges limiting long-term operation and costs of water processing. One of the problematic factors is the membrane fouling [32,100]. Besides advantages like high rejection of dissolved ions, low applied pressure, high permeate flux, processability on the commercial scale, and low operating temperature, the MD water processing remains energy intensive with high conductive heat loss [213,214]. According to the reported literature, the AGMD is more suitable to textile wastewater treatment compared to DCMD for its simplicity, higher thermal efficiencies, and low risk of the TP [215]. Nevertheless, this method results in low flux compared to other configurations. Although high fluxes are reported in DCMD, the process is limited to high membrane wettability. The SGMD requires more complex setups limiting is broad use and in contrast to other configurations. Also, SGMD has a higher risk of TP.

Development of scalable processes to fabricate membranes incorporated with nanoporous materials such as zeolites, metal-organic materials, and 2D materials is imperative. Currently, these membranes are at a relatively low technology readiness level. Interfacial polymerization is the most used technique to form ultrathin membranes for gas and water treatment. A recent review discusses opportunities and challenges associated with practical application of porous material at large scale and commercialization of membranes modified with nanoporous materials [216]. Some of the determining factors for potential commercialization include membrane selectivity and permeability, membrane synthesis cost, long-term stability as well as process reproducibility. Therefore, there is need to develop scalable fabrication methods which result in reproducible membranes in terms of structure and separation performance.

Many sources demonstrate application of MD on the model and real wastewater solutions containing different concentration of dyes, where the application is limited to the solutions below or equal 100 ppm of certain dye. The increase in dye concentration cause a decay in permeate flux [217]. Another challenge is surface tension of the membrane and wetting in presence of surfactants commonly present in textile wastewaters [48,218]. Formation of cohesive interactions between the hydrophilic groups of surfactant molecules in the feed affect permeation flux, thus necessitating the wetting investigation during MD treatment of textile industry wastewater [124,199,218]. Besides studies in the presence of surfactants, the improvement of the surface properties of the membrane towards superhydrophobicity is desired. Also, it is important to investigate steady state and operation times for each techniques [199]. Just in the same way, MD treatment of dyes requires effective and universal analytical models for particular membrane configurations for heat and mass transfer correlating to the specific dye. This is particularly important in treatment of environmental wastewater characterised varying pH, salinity, and presence of different chemicals [219]. Indeed, literature refers mathematical models developed for certain membrane configurations (flat sheet, spiral or hollow fibre) used in MD pilot units to

predict mass fluxes and compare them with measured water vapour fluxes [220]. However, extensive research is required.

To address the thermal efficiencies in MD, the research has geared towards evaluation of photothermal membrane distillation (PMD). This was encouraged by the large energy consumption with low thermal efficiency impeding the process application at energy off-grid areas [221,222]. The PMD utilizes the solar energy modification of the membrane to heat the feed solution by photothermal materials in situ. Technically, the photothermal materials are embedded into the membrane to generate the solar-based thermal energy. Technically, the temperature of the feed at the membrane interface is higher than the temperature of the bulk feed, thus enabling the large temperature difference and therefore the high vapour pressure gradient [223]. Various materials evaluated to convert light to heat include TiO_2, molybdenum disulfide (MoS_2), and MXenes (Ti_3C_2), CNTs, GO, and RGO [224]. Zhang et al. (2023) used carbonized lotus root as alternative cost effective photothermal materials to induce steam from the seawater via a solar simulator. The distillation process presented the flux of 0.90 $kg \cdot m^{-2} \cdot h^{-1}$ and GOR of 0.61 under 1 kWm^{-2} illumination [225]. Although utilization of photothermal materials have opened research direction towards cost-effective desalination processes, treatment of dye wastewater via PMD is rarely reported.

8. Conclusions

Membrane distillation (MD) emerged as an effective promising technology capable of treating industrial wastewater including textile. Previously reported studies advanced significant strides of MD process optimization, with a specific focus on membrane properties and operating parameters to improve rate of water recovery and dye removal efficiency. The MD facilitates water and dye separation through vapour-phase transport mechanisms where the porous hydrophobic

membrane permit passage of water vapour and volatile compounds while retaining the dye molecules. The current study comprehensively reviewed the MD treatment of various classes of dyes such as azo, reactive, and anthraquinone. Nonetheless, process challenges including membrane fouling, and energy optimizations require further considerations to enable practical implementation in textile wastewater management. To address these challenges, innovative approaches should focus on fouling mitigation strategies, improved membrane properties through surface modification. Thermal energy consumption requires critical attention in MD to assess its economic viability and environmental sustainability. As per previously reported studies, MD operation using low-grade or waste heat reduces the operations costs. However, some studies challenge the phenomenon of cost reduction upon use of low-grade energy or waste heat. For these reasons, research is geared towards module designs and fabrication of low-thermal conducting membranes. Also, in-situ detection of membrane fouling is required to enable an immediate mitigation. Among other technologies, artificial intelligence (AI) emerged as the modelling technology to improve process efficiency. However, AI evaluation in MD dye removal requires extensive research. Similarly, the emphasised need to use sustainable and environmentally friendly dye removal technologies, MD provides a promising avenue to address the water pollution caused by growing textile industries. Technically, the MD aligns with required principles of energy efficiency and zero liquid discharge. Upon further research and development efforts, coupled with advancements in process optimization, MD presented a great potential to treat dye-contaminated sources in a cost-effective and eco-friendly manner, thus ensuring cleaner and more sustainable water resources.

Acknowledgments

The authors would like to thank the University of the Witwatersrand and National Research Foundation (NRF-grant number: 132724) for funding this research work.

References

[1] V. Katheresan, J. Kansedo, S.Y. Lau, Efficiency of various recent wastewater dye removal methods : A review, J. Environ. Chem. Eng. 6 (2018) 4676–4697. https://doi.org/10.1016/j.jece.2018.06.060.

[2] S. Benkhaya, M. Souad, A. El Harfi, A review on classifications , recent synthesis and applications of textile dyes, Inorg. Chem. Commun. 115 (2020) 107891 Contents. https://doi.org/10.1016/j.inoche.2020.107891.

[3] M.A. Rauf, S. Hisaindee, Studies on solvatochromic behavior of dyes using spectral techniques, J. Mol. Struct. J. 1042 (2013) 45–56. https://doi.org/10.1016/j.molstruc.2013.03.050.

[4] S. Benkhaya, M. Souad, A. El Harfi, A review on classifications , recent synthesis and applications of textile dyes, Inorg. Chem. Commun. 115 (2020) 107891. https://doi.org/10.1016/j.inoche.2020.107891.

[5] C.D. Raman, S. Kanmani, Textile dye degradation using nano zero valent iron : A review, J. Environ. Manage. 177 (2016) 341–355. https://doi.org/10.1016/j.jenvman.2016.04.034.

[6] T.A. Nguyen, R. Juang, Treatment of waters and wastewaters containing sulfur dyes : A review, Chem. Eng. J. 219 (2013) 109–117. https://doi.org/10.1016/j.cej.2012.12.102.

[7] S. Zhang, W. Ma, B. Ju, N. Dang, M. Zhang, Continuous dyeing of cationised cotton with reactive dyes Coloration Technology, Color. Technol. 121 (2005) 183–186.

[8] L. Pei, J. Liu, J. Wang, Study of dichlorotriazine reactive dye hydrolysis in siloxane reverse micro-emulsion, J. Clean. Prod. 165 (2017) 994–1004. https://doi.org/10.1016/j.jclepro.2017.07.185.

[9] H. Xiao, T. Zhao, C. Li, M. Li, Eco-friendly approaches for dyeing multiple type of fabrics with cationic reactive dyes, J. Clean. Prod. 165 (2017) 1499–1507. https://doi.org/10.1016/j.jclepro.2017.07.174.

[10] M.M. Hassan, C.M. Carr, A critical review on recent advancements of the removal of reactive dyes from dyehouse ef fl uent by ion-exchange adsorbents, Chemosphere. 209 (2018) 201–219. https://doi.org/10.1016/j.chemosphere.2018.06.043.

[11] D. Rajkumar, J.G. Kim, Oxidation of various reactive dyes with in situ electro-generated active chlorine for textile dyeing industry wastewater treatment, J. Hazard. Mater. 136 (2006) 203–212. https://doi.org/10.1016/j.jhazmat.2005.11.096.

[12] C.R. Holkar, A.J. Jadhav, D. V Pinjari, N.M. Mahamuni, A.B. Pandit, A critical review on textile wastewater treatments : Possible approaches, J. Environ. Manage. 182 (2016) 351–366.

[13] C. Serra, M. Kogevinas, D.T. Silverman, D. Turuguet, A. Tardon, A. Carrato, G. Castan, F. Fernandez, P. Stewart, F.G. Benavides, Work in the textile industry in Spain and bladder cancer, Occup. Environ. Med. 65 (2008) 552–559. https://doi.org/10.1136/oem.2007.035667.

[14] Z. Singh, P. Chadha, Textile industry and occupational cancer, J. Occup. Med. Toxicolgy. 11 (2016) 1–6. https://doi.org/10.1186/s12995-016-0128-3.

[15] E. Helaskoski, H. Suojalehto, H. Virtanen, L. Airaksinen, K. Outi, M. Aalto-Korte, Kristiina Pesonen, Occupational asthma , rhinitis , and contact urticaria caused by oxidative hair

dyes in hairdressers, Ann Allergy Asthma Immunol. 112 (2014) 46–52. https://doi.org/10.1016/j.anai.2013.10.002.

[16] R. Fried, I. Oprea, K. Fleck, F. Rudrof, Biogenic colourants in the textile industry – a promising and sustainable alternative to synthetic dyes, Green Chem. 24 (2022) 13–35. https://doi.org/10.1039/d1gc02968a.

[17] J. Rovira, J.L. Domingo, Human health risks due to exposure to inorganic and organic chemicals from textiles: A review, Environ. Res. 168 (2019) 62–69. https://doi.org/10.1016/j.envres.2018.09.027.

[18] R. Kant, Textile dyeing industry an environmental hazard, Nat. Sci. 4 (2012) 22–26. https://doi.org/10.4236/ns.2012.41004.

[19] R. Al-Tohamy, S.S. Ali, F. Li, K.M. Okasha, Y.A.G. Mahmoud, T. Elsamahy, H. Jiao, Y. Fu, J. Sun, A critical review on the treatment of dye-containing wastewater: Ecotoxicological and health concerns of textile dyes and possible remediation approaches for environmental safety, Ecotoxicol. Environ. Saf. 231 (2022) 113160. https://doi.org/10.1016/j.ecoenv.2021.113160.

[20] S. Samsami, M. Mohamadi, M.H. Sarrafzadeh, E.R. Rene, M. Firoozbahr, Recent advances in the treatment of dye-containing wastewater from textile industries: Overview and perspectives, Process Saf. Environ. Prot. 143 (2020) 138–163. https://doi.org/10.1016/j.psep.2020.05.034.

[21] M. Khayet, Membranes and theoretical modeling of membrane distillation: A review, Adv. Colloid Interface Sci. 164 (2011) 56–88. https://doi.org/10.1016/j.cis.2010.09.005.

[22] M.M.A. Shirazi, A. Kargari, A Review on Applications of Membrane Distillation (MD) Process for Wastewater Treatment, J. Membr. Sci. Res. 1 (2015) 101–112.

[23] E. Drioli, F. Matera, Membrane distillation in the textile wastewater treatment, Desalination. 83 (1991) 209–224.

[24] F. Banat, S. A-asheh, M. Qtaishat, Treatment of waters colored with methylene blue dye by vacuum membrane distillation, Desalination. 174 (2005) 87–96. https://doi.org/10.1016/j.desal.2004.09.004.

[25] A. Criscuoli, J. Zhong, A. Figoli, M.C. Carnevale, R. Huang, E. Drioli, Treatment of dye solutions by vacuum membrane distillation, Water Res. 42 (2008) 5031–5037. https://doi.org/10.1016/j.watres.2008.09.014.

[26] T. Mpala, I. Chimanlal, H. Richards, A. Etale, L.N. Nthunya, Hybrid membrane processes equipped with crystallization unit for a simultaneous recovery of freshwater and minerals from saline wastewater, in: Innov. Trends Remov. Refract. Pollut. from Pharm. Wastewater H, Elsevier, Netherlands, 2024: pp. 71–91. https://doi.org/10.1016/B978-0-323-99278-7.00010-9.

[27] H. Ramlow, V. Hugo, M. Correa, R. Antonio, F. Machado, A. Cristiane, K. Bierhalz, C. Marangoni, Intensification of water reclamation from textile dyeing wastewater using thermal membrane technologies – Performance comparison of vacuum membrane distillation and thermopervaporation, Chem. Eng. Process. Process Intensif. 146 (2019) 1–7. https://doi.org/10.1016/j.cep.2019.107695.

[28] S. Leaper, A. Abdel-karim, T.A. Gad-allah, P. Gorgojo, Air-gap membrane distillation as a one-step process for textile wastewater treatment, Chem. Eng. J. 360 (2019) 1330–1340. https://doi.org/10.1016/j.cej.2018.10.209.

[29] M. Laqbaqbi, M.C. García-payo, M. Khayet, J. El Kharraz, M. Chaouch, Application of direct contact membrane distillation for textile wastewater treatment and fouling study, Sep. Purif.

Technol. 209 (2019) 815–825. https://doi.org/10.1016/j.seppur.2018.09.031.

[30] L. Eykens, K. De Sitter, C. Dotremont, L. Pinoy, B. Van der Bruggen, Membrane synthesis for membrane distillation: A review, Sep. Purif. Technol. 182 (2017) 36–51. https://doi.org/10.1016/j.seppur.2017.03.035.

[31] N.M. Mokhtar, W.J. Lau, A.F. Ismail, The potential of membrane distillation in recovering water from hot dyeing solution, J. Water Process Eng. 2 (2014) 71–78. https://doi.org/10.1016/j.jwpe.2014.05.006.

[32] N.M. Mokhtara, W.J. Lau, A.F. Ismailb, S. Kartohardjonoc, S.O. Laid, H.C. Teoh, The potential of direct contact membrane distillation for industrial textile wastewater treatment using PVDF-Cloisite 15A nanocomposite, Chem. Eng. Res. Des. 111 (2016) 284–293. https://doi.org/10.1016/j.cherd.2016.05.018.

[33] R. Suresh, S. Rajendran, L. Gnanasekaran, P.L. Show, M. Soto-moscoso, Modified poly(vinylidene fluoride) nanomembranes for dye removal from water – A review, Chemosphere. 322 (2023) 138152. https://doi.org/10.1016/j.chemosphere.2023.138152.

[34] I. Chimanlal, L.N. Nthunya, O.T. Mahlangu, B. Kirkebæk, A. Ali, C.A. Quist-jensen, H. Richards, Nanoparticle-Enhanced PVDF Flat-Sheet Membranes for Seawater Desalination in Direct Contact Membrane Distillation, Membranes (Basel). 13 (2023) 1–17. https://doi.org/10.3390/membranes13030317.

[35] I. Chimanlal, L.N. Nthunya, C. Quist-Jensen, H. Richards, Resource recovery from acid mine drainage in membrane distillation crystallization, Front. Membr. Sci. Technol. 2 (2023) 1–10. https://doi.org/10.3389/frmst.2023.1247276.

[36] M.E. Lousada, E.A. Lopez Maldonado, L.N. Nthunya, A. Mosai, M.L.P. Antunes, L.F. Fraceto, E. Baigorria, Nanoclays and mineral derivates applied to pesticide water

remediation, J. Contam. Hydrol. 259 (2023) 104264. https://doi.org/10.1016/j.jconhyd.2023.104264.

[37] E. Gontarek-castro, R. Castro-muñoz, M. Lieder, New insights of nanomaterials usage toward superhydrophobic membranes for water desalination via membrane distillation: A review, Crit. Rev. Environ. Sci. Technol. 52 (2022) 2104–2149. https://doi.org/10.1080/10643389.2021.1877032.

[38] O.T. Mahlangu, T.I. Nkambule, B.B. Mamba, F.I. Hai, Strategies for mitigating challenges associated with trace organic compound removal by high-retention membrane bioreactors (HR-MBRs), Npj Clean Water. 7 (2024) 1–39. https://doi.org/10.1038/s41545-024-00313-w.

[39] E. Gontarek-castro, R. Castro-muñoz, Membrane distillation assisting food production processes of thermally sensitive food liquid items: a review, Crit. Rev. Food Sci. Nutr. (2023). https://doi.org/10.1080/10408398.2022.2163223.

[40] E. Gontarek-castro, R. Castro-Munoz, How to make membrane distillation greener: a review of environmentally friendly and sustainable aspects, Green Chem. 26 (2024) 164–185. https://doi.org/10.1039/d3gc03377e.

[41] M. Zamidi, V. Martin-gil, T. Supinkova, P. Lambert, Novel MMM using CO2 selective SSZ-16 and high-performance 6FDA- polyimide for CO2/CH4 separation, Sep. Purif. Technol. 254 (2021) 117582. https://doi.org/10.1016/j.seppur.2020.117582.

[42] M. Zamidi, M. Malankowska, R. Castro-mu, A new relevant membrane application: CO2 direct air capture (DAC), Chem. Eng. J. 446 (2022) 137047. https://doi.org/10.1016/j.cej.2022.137047.

[43] Castro-Munoz Roberto, K.V. Agrawal, J. Coronas, Ultrathin permselective membranes: the

latent way for efficient gas separation, RSC Adv. 10 (2020) 12653–12670. https://doi.org/10.1039/d0ra02254c.

[44] M.Z. Ahmad, H. Pelletier, V. Martin-gil, R. Castro-muñoz, V. Fila, Chemical Crosslinking of 6FDA-ODA and 6FDA-ODA: DABA for Improved CO2/CH4 Separation, Membranes (Basel). 8 (2018) 67. https://doi.org/10.3390/membranes8030067.

[45] A. Jain, M.Z. Ahmad, A. Link, V. Martin-gil, R. Castro-muñoz, P. Izak, W. Hintz, V. Fila, 6FDA-DAM: DABA Co-Polyimide Mixed Matrix Membranes with GO and ZIF-8 Mixtures for Effective CO2/CH4 Separation, Nanomaterials. 11 (2021) 668.

[46] A.K. An, J. Guo, E.J. Lee, S. Jeong, Y. Zhao, Z. Wang, T.O. Leiknes, PDMS/PVDF hybrid electrospun membrane with superhydrophobic property and drop impact dynamics for dyeing wastewater treatment using membrane distillation, J. Memb. Sci. 525 (2017) 57–67. https://doi.org/10.1016/j.memsci.2016.10.028.

[47] M.M.A. Shirazi, A. Kargari, M. Tabatabaei, Evaluation of commercial PTFE membranes in desalination by direct contact membrane distillation, Chem. Eng. Process. Process Intensif. 76 (2014) 16–25. https://doi.org/10.1016/j.cep.2013.11.010.

[48] G. Yang, J. Zhang, M. Peng, E. Du, Y. Wang, G. Shan, L. Ling, H. Ding, S. Gray, Z. Xie, A mini review on antiwetting studies in membrane distillation for textile wastewater treatment, Processes. 9 (2021) 1–16. https://doi.org/10.3390/pr9020243.

[49] J.V. García, N. Dow, N. Milne, J. Zhang, L. Naidoo, S. Gray, M. Duke, Membrane distillation trial on textile wastewater containing surfactants using hydrophobic and hydrophilic-coated polytetrafluoroethylene (PTFE) membranes, Membranes (Basel). 8 (2018) 1–15. https://doi.org/10.3390/membranes8020031.

[50] L.N. Nthunya, L. Gutierrez, A.R. Verliefde, S.D. Mhlanga, Enhanced flux in direct contact

membrane distillation using superhydrophobic PVDF nanofibre membranes embedded with organically modified SiO2 nanoparticles, J. Chem. Technol. Biotechnol. 94 (2019) 2826–2837. https://doi.org/10.1002/jcbt.6104.

[51] L.N. Nthunya, L. Gutierrez, S. Derese, N. Edward, A.R. Verliefde, B. Mamba, S.D. Mhlanga, A review of nanoparticle-enhanced membrane distillation membranes : membrane synthesis and applications in water treatment, Chem. Technol. Biotechnol. 94 (2019) 2757–2771. https://doi.org/10.1002/jctb.5977.

[52] M.M.A. Shirazi, S. Bazgir, F. Meshkani, A dual-layer, nanofibrous styrene-acrylonitrile membrane with hydrophobic/hydrophilic composite structure for treating the hot dyeing effluent by direct contact membrane distillation, Chem. Eng. Res. Des. 164 (2020) 125–146. https://doi.org/10.1016/j.cherd.2020.09.030.

[53] A. Yadav, R.V. Patel, P.K. Labhasetwar, V.K. Shahi, Novel MIL101(Fe) impregnated poly(vinylidene fluoride-co-hexafluoropropylene) mixed matrix membranes for dye removal from textile industry wastewater, J. Water Process Eng. 43 (2021) 102317. https://doi.org/10.1016/j.jwpe.2021.102317.

[54] Q. Huang, Y. Huang, C. Xiao, Y. You, C. Zhang, Self-Cleaning Function for Vacuum Membrane Distillation, J. Memb. Sci. 534 (2017) 73–82. https://doi.org/10.1016/j.memsci.2017.04.015.

[55] H. Li, X. Feng, W. Shi, H. Zhang, Q. Du, L. Qin, X. Qin, Dye removal using hydrophobic polyvinylidene fluoride hollow fibre composite membrane by vacuum membrane distillation, Color. Technol. 135 (2019) 451–466. https://doi.org/10.1111/cote.12436.

[56] H. Li, X. Feng, Dye removal using hydrophobic polyvinylidene fluoride hollow fibre composite membrane by vacuum membrane distillation, Color. Technol. 135 (2019) 451–

466. https://doi.org/10.1111/cote.12436.

[57] S.A. Mousavi, Z. Arab Aboosadi, A. Mansourizadeh, B. Honarvar, Modification of porous polyetherimide hollow fiber membrane by dip-coating of Zonyl® BA for membrane distillation of dyeing wastewater, Water Sci. Technol. 83 (2021) 3092–3109. https://doi.org/10.2166/wst.2021.201.

[58] S. Xie, J. Du, X. Huang, A. Gu, S. Fang, R. Liu, D. Zou, J. Lin, M. Xie, S. Zhao, W. Ye, Water Recovery from Highly Saline Dye Wastewater by Membrane Distillation Using a Superhydrophobic SiO2/PVDF Membrane, ACS ES T Water. 3 (2023) 1893–1901. https://doi.org/10.1021/acsestwater.2c00519.

[59] F. Russo, R. Castro-muñoz, F. Galiano, A. Figoli, Unprecedented preparation of porous Matrimid ® 5218 membranes, J. Memb. Sci. 585 (2019) 166–174. https://doi.org/10.1016/j.memsci.2019.05.036.

[60] I. Ounifi, Y. Guesmi, C. Ursino, R. Castro-Muñoz, H. Agougui, M. Jabli, A. Hafiane, A. Figoli, E. Ferjani, Synthesis and Characterization of a Thin-Film Composite Nanofiltration Membrane Based on Polyamide-Cellulose Acetate: Application for Water Purification, J. Polym. Environ. 30 (2022) 707–718. https://doi.org/10.1007/s10924-021-02233-z.

[61] L. Loreti, R. Castro-mu, Ongoing progress on novel nanocomposite membranes for the separation of heavy metals from contaminated water, Chemosphere. 270 (2021) 129421. https://doi.org/10.1016/j.chemosphere.2020.129421.

[62] S. Parani, O.S. Oluwafemi, Membrane distillation: Recent configurations, membrane surface engineering, and applications, Membranes (Basel). 11 (2021) 1–26. https://doi.org/10.3390/membranes11120934.

[63] J. Zhang, J. De Li, M. Duke, M. Hoang, Z. Xie, A. Groth, C. Tun, S. Gray, Influence of

module design and membrane compressibility on VMD performance, J. Memb. Sci. 442 (2013) 31–38. https://doi.org/10.1016/j.memsci.2013.04.028.

[64] M.A. Izquierdo-Gil, G. Jonsson, Factors affecting flux and ethanol separation performance in vacuum membrane distillation (VMD), J. Memb. Sci. 214 (2003) 113–130. https://doi.org/10.1016/S0376-7388(02)00540-9.

[65] I.A. Said, T. Chomiak, J. Floyd, Q. Li, Sweeping gas membrane distillation (SGMD) for wastewater treatment, concentration, and desalination: A comprehensive review, Chem. Eng. Process. - Process Intensif. 153 (2020) 107960. https://doi.org/10.1016/j.cep.2020.107960.

[66] O.T. Mahlangu, L.N. Nthunya, M.M. Motsa, E. Morifi, H. Richards, B.B. Mamba, Fouling of high pressure-driven NF and RO membranes in desalination processes: Mechanisms and implications on salt rejection, Chem. Eng. Res. Des. 199 (2023) 268–295. https://doi.org/10.1016/j.cherd.2023.09.037.

[67] L.N. Nthunya, M.F. Bopape, O.T. Mahlangu, B.B. Mamba, B. Van der Bruggen, C.A. Quist-Jensen, H. Richards, Fouling, performance and cost analysis of membrane-based water desalination technologies: A critical review, J. Environ. Manage. 301 (2022) 113922. https://doi.org/10.1016/j.jenvman.2021.113922.

[68] T.O. Mahlangu, J.M. Thwala, B.B. Mamba, A. D'Haese, A.R.D. Verliefde, Factors governing combined fouling by organic and colloidal foulants in cross-flow nanofiltration, J. Memb. Sci. 491 (2015) 53–62. https://doi.org/10.1016/j.memsci.2015.03.021.

[69] E. Salehi, R. Castro-mu, Zeolitic imidazolate framework (ZIF-8) modified cellulose acetate NF membranes for potential water treatment application, 299 (2023). https://doi.org/10.1016/j.carbpol.2022.120230.

[70] J.R.A. Cosme, R. Castro-mun, Recent Advances in Nanocomposite Membranes for Organic Compound Remediation from Potable Waters, (2023) 112–132. https://doi.org/10.1002/cben.202200017.

[71] O.T. Mahlangu, M.M. Motsa, F.I. Hai, B.B. Mamba, Role of Membrane–Solute Affinity Interactions in Carbamazepine Rejection and Resistance to Organic Fouling by Nano-Engineered UF/PES Membranes, Membranes (Basel). 13 (2023) 744. https://doi.org/10.3390/membranes13080744.

[72] D. Pichardo-romero, Z.P. Garcia-arce, A. Zavala-ram, R. Castro-muñoz, Current Advances in Biofouling Mitigation in Membranes for Water Treatment : An Overview, Processes. 8 (2020) 182. https://doi.org/doi:10.3390/pr8020182.

[73] T.J. Mpala, A. Etale, H. Richards, L.N. Nthunya, Biofouling phenomena in membrane distillation : mechanisms and mitigation strategies, Environ. Sci. Adv. 2 (2022) 39–54. https://doi.org/10.1039/d2va00161f.

[74] S. Du, P. Zhao, L. Wang, G. He, X. Jiang, Progresses of advanced anti-fouling membrane and membrane processes for high salinity wastewater treatment, Results Eng. 17 (2023) 100995. https://doi.org/10.1016/j.rineng.2023.100995.

[75] N.M. Mokhtar, W.J. Lau, A.F. Ismail, W. Youravong, W. Khongnakorn, K. Lertwittayanon, Performance evaluation of novel PVDF-Cloisite 15A hollow fiber composite membranes for treatment of effluents containing dyes and salts using membrane distillation, RSC Adv. 5 (2015) 38011–38020. https://doi.org/10.1039/c5ra00182j.

[76] H. Yang, X. Yu, J. Liu, Z. Tang, T. Huang, Z. Wang, Y. Zhong, Z. Long, L. Wang, A Concise Review of Theoretical Models and Numerical Simulations of Membrane Fouling, Water. 14 (2022) 3537. https://doi.org/10.3390/w14213537.

[77] N.H.H. Hairom, A.W. Mohammad, A.A.H. Kadhum, Nanofiltration of hazardous Congo red dye: Performance and flux decline analysis, J. Water Process Eng. 4 (2014) 99–106. https://doi.org/10.1016/j.jwpe.2014.09.008.

[78] W. Zhang, L. Ding, Investigation of membrane fouling mechanisms using blocking models in the case of shear-enhanced ultrafiltration, Sep. Purif. Technol. 141 (2015) 160–169. https://doi.org/10.1016/j.seppur.2014.11.041.

[79] H. Xu, K. Xiao, X. Wang, S. Liang, C. Wei, X. Wen, X. Huang, Outlining the Roles of Membrane-Foulant and Foulant-Foulant Interactions in Organic Fouling During Microfiltration and Ultrafiltration: A Mini-Review, Front. Chem. 8 (2020) 1–14. https://doi.org/10.3389/fchem.2020.00417.

[80] M.A. Ahmed, S. Amin, A.A. Mohamed, Fouling in reverse osmosis membranes: monitoring, characterization, mitigation strategies and future directions, Heliyon. 9 (2023) e14908 Contents. https://doi.org/10.1016/j.heliyon.2023.e14908.

[81] H. Ramlow, R.A.F. Machado, A.C.K. Bierhalz, C. Marangoni, Direct contact membrane distillation applied to wastewaters from different stages of the textile process, Chem. Eng. Commun. 207 (2020) 1062–1073. https://doi.org/10.1080/00986445.2019.1640683.

[82] L. Fortunato, H. Elcik, B. Blankert, N. Ghaffour, J. Vrouwenvelder, Textile dye wastewater treatment by direct contact membrane distillation: Membrane performance and detailed fouling analysis, J. Memb. Sci. 636 (2021) 119552. https://doi.org/10.1016/j.memsci.2021.119552.

[83] A. Haleem, A. Shafiq, S.Q. Chen, M. Nazar, A Comprehensive Review on Adsorption, Photocatalytic and Chemical Degradation of Dyes and Nitro-Compounds over Different Kinds of Porous and Composite Materials, Molecules. 28 (2023).

https://doi.org/10.3390/molecules28031081.

[84] S. Yang, S. Abdalkareem Jasim, D. Bokov, S. Chupradit, A.T. Nakhjiri, A.S. El-Shafay, Membrane distillation technology for molecular separation: A review on the fouling, wetting and transport phenomena, J. Mol. Liq. 349 (2022) 118115. https://doi.org/10.1016/j.molliq.2021.118115.

[85] M.O. Aijaz, M.R. Karim, M.H.D. Othman, U.A. Samad, Anti-fouling/wetting electrospun nanofibrous membranes for membrane distillation desalination: A comprehensive review, Desalination. 553 (2023) 116475. https://doi.org/10.1016/j.desal.2023.116475.

[86] P.G. shekhi Abadi, M. Irani, L.R. Rad, Mechanisms of the removal of the metal ions, dyes, and drugs from wastewaters by the electrospun nanofiber membranes, J. Taiwan Inst. Chem. Eng. 143 (2023) 104625. https://doi.org/10.1016/j.jtice.2022.104625.

[87] T. Chidambaram, Y. Oren, M. Noel, Fouling of nanofiltration membranes by dyes during brine recovery from textile dye bath wastewater, Chem. Eng. J. 262 (2015) 156–168. https://doi.org/10.1016/j.cej.2014.09.062.

[88] L.M. Camacho, L. Dumée, J. Zhang, J. de Li, M. Duke, J. Gomez, S. Gray, Advances in membrane distillation for water desalination and purification applications, Water. 5 (2013) 94–196. https://doi.org/10.3390/w5010094.

[89] A.S. Reddy, S. Kalla, Z.V.P. Murthy, Textile wastewater treatment via membrane distillation, Environ. Eng. Res. 27 (2022) 1–16. https://doi.org/10.4491/eer.2021.228.

[90] R. de S. Silva, H. Ramlow, B. de C. Santos, H.B. Madalosso, R.A.F. Machado, C. Marangoni, Membrane Distillation: Experimental evaluation of Liquid Entry Pressure in commercial membranes with textile dye solutions, J. Water Process Eng. 44 (2021) 102339. https://doi.org/10.1016/j.jwpe.2021.102339.

[91] A.M. Hidalgo, G. León, M. Gómez, M.D. Murcia, E. Gómez, J.A. Macario, Removal of different dye solutions: A comparison study using a polyamide nf membrane, Membranes (Basel). 10 (2020) 1–16. https://doi.org/10.3390/membranes10120408.

[92] N.P. Khumalo, L.N. Nthunya, E. De Canck, S. Derese, A.R. Verliefde, A.T. Kuvarega, B.B. Mamba, S.D. Mhlanga, D.S. Dlamini, Congo red dye removal by direct membrane distillation using PVDF/PTFE membrane, Sep. Purif. Technol. 211 (2019) 578–586. https://doi.org/10.1016/j.seppur.2018.10.039.

[93] J. Hou, Y. Chen, W. Shi, C. Bao, X. Hu, Graphene oxide/methylene blue composite membrane for dyes separation: Formation mechanism and separation performance, Appl. Surf. Sci. 505 (2020) 144145. https://doi.org/10.1016/j.apsusc.2019.144145.

[94] S. Parakala, S. Moulik, S. Sridhar, Effective separation of methylene blue dye from aqueous solutions by integration of micellar enhanced ultrafiltration with vacuum membrane distillation, Chem. Eng. J. 375 (2019) 122015. https://doi.org/10.1016/j.cej.2019.122015.

[95] S. Benkhaya, H. Lgaz, H. Tang, A. Altaee, S. Haida, V. Vatanpour, Y. Xiao, Investigating the effects of polypropylene-TiO2 loading on the performance of polysulfone/polyetherimide ultrafiltration membranes for azo dye removal: Experimental and molecular dynamics simulation, J. Water Process Eng. 56 (2023) 104317. https://doi.org/10.1016/j.jwpe.2023.104317.

[96] R.E. Elwardany, H. Shokry, A.A. Mustafa, A.E. Ali, Influence of the prepared activated carbon on cellulose acetate for malachite green dye removal from aqueous solution, Macromol. Res. 31 (2023) 1043–1060. https://doi.org/10.1007/s13233-023-00187-w.

[97] S. Elgharbi, A. Boubakri, S. Bouguecha, H. Bilel, S.I. Matalka, A. Hafiane, Membrane

Distillation for Methylene Blue Dye Removal from Wastewater: Investigating Process Optimization and Membrane Wettability, Arab. J. Sci. Eng. (2024). https://doi.org/10.1007/s13369-024-08756-6.

[98] A.K. An, J. Guo, S. Jeong, E.J. Lee, S.A.A. Tabatabai, T.O. Leiknes, High flux and antifouling properties of negatively charged membrane for dyeing wastewater treatment by membrane distillation, Water Res. 103 (2016) 362–371. https://doi.org/10.1016/j.watres.2016.07.060.

[99] H. Ramlow, C. D'Ávila Kramer Cavalcanti, R.A.F. Machado, A.C. Krause Bierhalz, C. Marangoni, Direct Contact Membrane Distillation Applied to Colored Reactive or Disperse Dye Solutions, Chem. Eng. Technol. 42 (2019) 1045–1052. https://doi.org/10.1002/ceat.201800468.

[100] M. Laqbaqbi, M.C. García-Payo, M. Khayet, J. El Kharraz, M. Chaouch, Application of direct contact membrane distillation for textile wastewater treatment and fouling study, Sep. Purif. Technol. 209 (2019) 815–825. https://doi.org/10.1016/j.seppur.2018.09.031.

[101] N.M. Mokhtar, W.J. Lau, A.F. Ismail, S. Kartohardjono, S.O. Lai, H.C. Teoh, The potential of direct contact membrane distillation for industrial textile wastewater treatment using PVDF-Cloisite 15A nanocomposite membrane, Chem. Eng. Res. Des. 111 (2016) 284–293. https://doi.org/10.1016/j.cherd.2016.05.018.

[102] Z.S. Tai, M.H.D. Othman, K.N. Koo, J. Jaafar, Critical review on membrane designs for enhanced flux performance in membrane distillation, Desalination. 553 (2023) 116484. https://doi.org/10.1016/j.desal.2023.116484.

[103] A. Charfi, F. Tibi, J. Kim, J. Hur, J. Cho, Organic fouling impact in a direct contact membrane distillation system treating wastewater: Experimental observations and

modeling approach, Membranes (Basel). 11 (2021) 1–12. https://doi.org/10.3390/membranes11070493.

[104] N. Alsawaftah, W. Abuwatfa, N. Darwish, G. Husseini, A comprehensive review on membrane fouling: Mathematical modelling, prediction, diagnosis, and mitigation, Water (Switzerland). 13 (2021). https://doi.org/10.3390/w13091327.

[105] A. Alkhatib, M.A. Ayari, A.H. Hawari, Fouling mitigation strategies for different foulants in membrane distillation, Chem. Eng. Process. - Process Intensif. 167 (2021) 108517. https://doi.org/10.1016/j.cep.2021.108517.

[106] S.A. Mousavi, Z. Arab Aboosadi, A. Mansourizadeh, B. Honarvar, Modification of porous polyetherimide hollow fiber membrane by dip-coating of Zonyl® BA for membrane distillation of dyeing wastewater, Water Sci. Technol. 83 (2021) 3092–3109. https://doi.org/10.2166/wst.2021.201.

[107] M. Adel, T. Nada, S. Amin, T. Anwar, A.A. Mohamed, Characterization of fouling for a full-scale seawater reverse osmosis plant on the Mediterranean sea: membrane autopsy and chemical cleaning efficiency, Groundw. Sustain. Dev. 16 (2022) 100704. https://doi.org/10.1016/j.gsd.2021.100704.

[108] W.J. Lim, B.S. Ooi, Applications of responsive hydrogel to enhance the water recovery via membrane distillation and forward osmosis: A review, J. Water Process Eng. 47 (2022) 102828. https://doi.org/10.1016/j.jwpe.2022.102828.

[109] H. Li, W. Shi, Q. Du, S. Huang, H. Zhang, R. Zhou, X. Qin, Removal of high concentration Congo red by hydrophobic PVDF hollow fiber composite membrane coated with a loose and porous ZIF-71PVDF layer through vacuum membrane distillation, J. Ind. Text. 51 (2022) 7641S-7673S. https://doi.org/10.1177/1528083720967075.

[110] L.N. Nthunya, L. Gutierrez, N. Khumalo, S. Derese, B.B. Mamba, A.R. Verliefde, S.D. Mhlanga, Superhydrophobic PVDF nano fibre membranes coated with an organic fouling resistant hydrophilic active layer for direct-contact membrane distillation, Colloids Surfaces A. 575 (2019) 363–372. https://doi.org/10.1016/j.colsurfa.2019.05.031.

[111] L.N. Nthunya, L. Gutierrez, E.N. Nxumalo, A.R. Verliefde, S.D. Mhlanga, M.S. Onyango, f-MWCNTs / AgNPs-coated superhydrophobic PVDF nanofibre membrane for organic, colloidal, and biofouling mitigation in direct contact membrane distillation, J. Environ. Chem. Eng. 8 (2020) 103654. https://doi.org/10.1016/j.jece.2020.103654.

[112] T.J. Mpala, M.H. Serepa-dlamini, A. Etale, H. Richards, L.N. Nthunya, Cellulose nanocrystal-mediated synthesis of silver nanoparticles via microwave assisted method for biofouling control in membrane distillation, Mater. Today Commun. 34 (2023) 105028. https://doi.org/10.1016/j.mtcomm.2022.105028.

[113] S. Maity, B. Mishra, K. Nayak, N.C. Dubey, B.P. Tripathi, Zwitterionic microgel based anti(-bio)fouling smart membranes for tunable water filtration and molecular separation, Mater. Today Chem. 24 (2022) 100779. https://doi.org/10.1016/j.mtchem.2022.100779.

[114] Y.H. Huang, M.J. Wang, T.S. Chung, Zwitterionic poly(sulfobetaine methacrylate-co-acrylic acid) assisted simultaneous anti-wetting and anti-fouling membranes for membrane distillation, Desalination. 555 (2023) 116527. https://doi.org/10.1016/j.desal.2023.116527.

[115] M.M.A. Shirazi, S. Bazgir, F. Meshkani, A novel dual-layer, gas-assisted electrospun, nanofibrous SAN4-HIPS membrane for industrial textile wastewater treatment by direct contact membrane distillation (DCMD), J. Water Process Eng. 36 (2020) 101315. https://doi.org/10.1016/j.jwpe.2020.101315.

[116] L. Liu, Z. Xiao, Y. Liu, X. Li, H. Yin, A. Volkov, T. He, Understanding the fouling/scaling

resistance of superhydrophobic/omniphobic membranes in membrane distillation, Desalination. 499 (2021) 114864. https://doi.org/10.1016/j.desal.2020.114864.

[117] A. Yadav, P. Sharma, A.B. Panda, V.K. Shahi, Photocatalytic TiO2 incorporated PVDF-co-HFP UV-cleaning mixed matrix membranes for effective removal of dyes from synthetic wastewater system via membrane distillation, J. Environ. Chem. Eng. 9 (2021) 105904. https://doi.org/10.1016/j.jece.2021.105904.

[118] M.R. Choudhury, N. Anwar, D. Jassby, M.S. Rahaman, Fouling and wetting in the membrane distillation driven wastewater reclamation process – A review, Adv. Colloid Interface Sci. 269 (2019) 370–399. https://doi.org/10.1016/j.cis.2019.04.008.

[119] R. de S. Silva, C.D.Á.K. Cavalcanti, R. de C.S.C. Valle, R.A.F. Machado, C. Marangoni, Understanding the effects of operational conditions on the membrane distillation process applied to the recovery of water from textile effluents, Process Saf. Environ. Prot. 145 (2021) 285–292. https://doi.org/10.1016/j.psep.2020.08.022.

[120] A. Criscuoli, J. Zhong, A. Figoli, M.C. Carnevale, R. Huang, E. Drioli, Treatment of dye solutions by vacuum membrane distillation, Water Res. 42 (2008) 5031–5037. https://doi.org/10.1016/j.watres.2008.09.014.

[121] Z. Yan, Y. Jiang, L. Liu, Z. Li, X. Chen, M. Xia, G. Fan, A. Ding, Membrane distillation for wastewater treatment: A mini Review, Water. 13 (2021) 1–28. https://doi.org/10.3390/w13243480.

[122] I. Hitsov, K. De Sitter, C. Dotremont, I. Nopens, Economic modelling and model-based process optimization of membrane distillation, Desalination. 436 (2018) 125–143. https://doi.org/10.1016/j.desal.2018.01.038.

[123] W. Qin, Z. Xie, D. Ng, Y. Ye, X. Ji, S. Gray, J. Zhang, Comparison of colloidal silica involved

fouling behavior in three membrane distillation configurations using PTFE membrane, Water Res. 130 (2018) 343–352. https://doi.org/10.1016/j.watres.2017.12.002.

[124] N. Dow, J. Villalobos García, L. Niadoo, N. Milne, J. Zhang, S. Gray, M. Duke, Demonstration of membrane distillation on textile waste water assessment of long term performance, membrane cleaning and waste heat integration, Environ. Sci. Water Res. Technol. 3 (2017) 433–449. https://doi.org/10.1039/c6ew00290k.

[125] K. Manzoor, S.J. Khan, M. Yasmeen, Y. Jamal, M. Arshad, Assessment of anaerobic membrane distillation bioreactor hybrid system at mesophilic and thermophilic temperatures treating textile wastewater, J. Water Process Eng. 46 (2022) 102603. https://doi.org/10.1016/j.jwpe.2022.102603.

[126] W. Shi, T. Li, Y. Tian, H. Li, M. Fan, H. Zhang, X. Qin, An innovative hollow fiber vacuum membrane distillation-crystallization (VMDC) coupling process for dye house effluent separation to reclaim fresh water and salts, J. Clean. Prod. 337 (2022) 130586. https://doi.org/10.1016/j.jclepro.2022.130586.

[127] H. Julian, Y. Ye, H. Li, V. Chen, Scaling mitigation in submerged vacuum membrane distillation and crystallization (VMDC) with periodic air-backwash, J. Memb. Sci. 547 (2018) 19–33. https://doi.org/10.1016/j.memsci.2017.10.035.

[128] A. Abdel-Karim, S. Leaper, C. Skuse, G. Zaragoza, M. Gryta, P. Gorgojo, Membrane cleaning and pretreatments in membrane distillation – a review, Chem. Eng. J. 422 (2021) 129696. https://doi.org/10.1016/j.cej.2021.129696.

[129] C.X.H. Su, L.W. Low, T.T. Teng, Y.S. Wong, Combination and hybridisation of treatments in dye wastewater treatment: A review, J. Environ. Chem. Eng. 4 (2016) 3618–3631. https://doi.org/10.1016/j.jece.2016.07.026.

[130] I. Ibrar, S. Yadav, O. Naji, A.A. Alanezi, N. Ghaffour, S. Déon, S. Subbiah, A. Altaee, Development in forward Osmosis-Membrane distillation hybrid system for wastewater treatment, Sep. Purif. Technol. 286 (2022) 120498. https://doi.org/10.1016/j.seppur.2022.120498.

[131] Q. Ge, P. Wang, C. Wan, T.-S. Chung, Polyelectrolyte-Promoted Forward Osmosis – Membrane Distillation (FO – MD) Hybrid Process for Dye Wastewater Treatment, Environ. Sci. Technol. 46 (2012) 6236–6243. https://doi.org/10.1021/es300784h.

[132] M. Li, K. Li, L. Wang, X. Zhang, Feasibility of concentrating textile wastewater using a hybrid forward osmosis-membrane distillation (FO-MD) process: Performance and economic evaluation, Water Res. 172 (2020) 115488. https://doi.org/10.1016/j.watres.2020.115488.

[133] X. Wu, S. Ma, D. Ng, D. Acharya, L. Fan, Z. Xie, Enhancing water recovery through integrated graphene oxide-modified forward osmosis and membrane distillation for real textile wastewater treatment, J. Environ. Chem. Eng. 12 (2024) 112512. https://doi.org/10.1016/j.jece.2024.112512.

[134] M. Nadimi, M. Shahrooz, R. Wang, X. Yang, M.C. Duke, Process intensification with reactive membrane distillation: A review of hybrid and integrated processes, Desalination. 573 (2024) 117182. https://doi.org/10.1016/j.desal.2023.117182.

[135] S. Mozia, A.W. Morawski, M. Toyoda, M. Inagaki, Effectiveness of photodecomposition of an azo dye on a novel anatase-phase TiO2 and two commercial photocatalysts in a photocatalytic membrane reactor (PMR), Sep. Purif. Technol. 63 (2008) 386–391. https://doi.org/10.1016/j.seppur.2008.05.029.

[136] O. Makanjuola, B.S. Lalia, R. Hashaikeh, Thermoelectric heating and cooling for efficient

membrane distillation, Case Stud. Therm. Eng. 28 (2021). https://doi.org/10.1016/j.csite.2021.101540.

[137] Y. Elhenawy, M. Bassyouni, K. Fouad, A.M. Sandid, M.A.E.R. Abu-Zeid, T. Majozi, Experimental and numerical simulation of solar membrane distillation and humidification – dehumidification water desalination system, Renew. Energy. 215 (2023) 118915. https://doi.org/10.1016/j.renene.2023.118915.

[138] S.M. Alawad, A.E. Khalifa, Performance and energy evaluation of compact multistage air gap membrane distillation system: An experimental investigation, Sep. Purif. Technol. 268 (2021) 118594. https://doi.org/10.1016/j.seppur.2021.118594.

[139] H.C. Duong, P. Cooper, B. Nelemans, T.Y. Cath, L.D. Nghiem, Evaluating energy consumption of air gap membrane distillation for seawater desalination at pilot scale level, Sep. Purif. Technol. 166 (2016) 55–62. https://doi.org/10.1016/j.seppur.2016.04.014.

[140] J. Koschikowski, M. Wieghaus, M. Rommel, V.S. Ortin, B.P. Suarez, J.R. Betancort Rodríguez, Experimental investigations on solar driven stand-alone membrane distillation systems for remote areas, Desalination. 248 (2009) 125–131. https://doi.org/10.1016/j.desal.2008.05.047.

[141] F. Banat, N. Jwaied, M. Rommel, J. Koschikowski, M. Wieghaus, Desalination by a “compact SMADES” autonomous solarpowered membrane distillation unit, Desalination. 217 (2007) 29–37. https://doi.org/10.1016/j.desal.2006.11.028.

[142] G. Zaragoza, A. Ruiz-Aguirre, E. Guillén-Burrieza, Efficiency in the use of solar thermal energy of small membrane desalination systems for decentralized water production, Appl. Energy. 130 (2014) 491–499. https://doi.org/10.1016/j.apenergy.2014.02.024.

[143] J. Koschikowski, M. Wieghaus, M. Rommel, Solar thermal-driven desalination plants based

on membrane distillation, Desalination. 156 (2003) 295–304. https://doi.org/10.1016/S0011-9164(03)00360-6.

[144] K.S.S. Christie, T. Horseman, S. Lin, Energy efficiency of membrane distillation: Simplified analysis, heat recovery, and the use of waste-heat, Environ. Int. 138 (2020). https://doi.org/10.1016/j.envint.2020.105588.

[145] B.N. Tewodros, D.R. Yang, K. Park, Design Parameters of a Direct Contact Membrane Distillation and a Case Study of Its Applicability to Low-Grade Waste Energy, Membranes (Basel). 12 (2022) 1–31. https://doi.org/10.3390/membranes12121279.

[146] L.N. Nthunya, J. Pinier, A. Ali, C. Quist-jensen, H. Richards, Valorization of acid mine drainage into potable water and valuable minerals through membrane distillation crystallization, Sep. Purif. Technol. 334 (2024) 126084. https://doi.org/10.1016/j.seppur.2023.126084.

[147] A. Ali, J.H. Tsai, K.L. Tung, E. Drioli, F. Macedonio, Designing and optimization of continuous direct contact membrane distillation process, Desalination. 426 (2018) 97–107. https://doi.org/10.1016/j.desal.2017.10.041.

[148] M.R. Elmarghany, A.H. El-Shazly, M.S. Salem, M.N. Sabry, N. Nady, Thermal analysis evaluation of direct contact membrane distillation system, Case Stud. Therm. Eng. 13 (2019) 100377. https://doi.org/10.1016/j.csite.2018.100377.

[149] L. Song, B. Li, K.K. Sirkar, J.L. Gilron, Direct contact membrane distillation-based desalination: Novel membranes, devices, larger-scale studies, and a model, Ind. Eng. Chem. Res. 46 (2007) 2307–2323. https://doi.org/10.1021/ie0609968.

[150] M. Khayet, C. Cojocaru, Air gap membrane distillation: Desalination, modeling and optimization, Desalination. 287 (2012) 138–145.

https://doi.org/10.1016/j.desal.2011.09.017.

[151] M. Khayet, C. Cojocaru, A. Baroudi, Modeling and optimization of sweeping gas membrane distillation, Desalination. 287 (2012) 159–166. https://doi.org/10.1016/j.desal.2011.04.070.

[152] A. Ali, C.A. Quist-Jensen, F. Macedonio, E. Drioli, Optimization of module length for continuous direct contact membrane distillation process, Chem. Eng. Process. Process Intensif. 110 (2016) 188–200. https://doi.org/10.1016/j.cep.2016.10.014.

[153] H. Ramlow, R.A.F. Machado, C. Marangoni, Direct contact membrane distillation for textile wastewater treatment: A state of the art review, Water Sci. Technol. 76 (2017) 2565–2579. https://doi.org/10.2166/wst.2017.449.

[154] E.K. Summers, H.A. Arafat, J.H. Lienhard V, Energy efficiency comparison of single-stage membrane distillation (MD) desalination cycles in different configurations, Desalination. 290 (2012) 54–66. https://doi.org/10.1016/j.desal.2012.01.004.

[155] H.C. Duong, P. Cooper, B. Nelemans, T.Y. Cath, L.D. Nghiem, Optimising thermal efficiency of direct contact membrane distillation by brine recycling for small-scale seawater desalination, Desalination. 374 (2015) 1–9. https://doi.org/10.1016/j.desal.2015.07.009.

[156] J.G. Lee, S. Jeong, A.S. Alsaadi, N. Ghaffour, Influence of high range of mass transfer coefficient and convection heat transfer on direct contact membrane distillation performance, Desalination. 426 (2018) 127–134. https://doi.org/10.1016/j.desal.2017.10.034.

[157] J. Liu, W. Lin, H. Ren, A.K. Albdoor, F.I. Hai, Z. Ma, Multi-objective optimization of a direct contact membrane distillation regenerator for liquid desiccant regeneration, J. Clean. Prod. 373 (2022). https://doi.org/10.1016/j.jclepro.2022.133736.

[158] A. Ali, A. Criscuoli, F. Macedonio, E. Drioli, A comparative analysis of flat sheet and

1708 capillary membranes for membrane distillation applications, Desalination. 456 (2019) 1–
1709 12. https://doi.org/10.1016/j.desal.2019.01.006.

1710 [159] L. Martínez-Díez, M.I. Vázquez-González, F.J. Florido-Díaz, Study of membrane distillation
1711 using channel spacers, J. Memb. Sci. 144 (1998) 45–56. https://doi.org/10.1016/S0376-
1712 7388(98)00024-6.

1713 [160] M.N. Chernyshov, G.W. Meindersma, A.B. de Haan, Comparison of spacers for
1714 temperature polarization reduction in air gap membrane distillation, Desalination. 183
1715 (2005) 363–374. https://doi.org/10.1016/j.desal.2005.04.029.

1716 [161] L. Martínez, J.M. Rodríguez-Maroto, Characterization of membrane distillation modules
1717 and analysis of mass flux enhancement by channel spacers, J. Memb. Sci. 274 (2006)
1718 123–137. https://doi.org/10.1016/j.memsci.2005.07.045.

1719 [162] J. Phattaranawik, R. Jiraratananon, A.G. Fane, Effects of net-type spacers on heat and
1720 mass transfer in direct contact membrane distillation and comparison with ultrafiltration
1721 studies, J. Memb. Sci. 217 (2003) 193–206. https://doi.org/10.1016/S0376-
1722 7388(03)00130-3.

1723 [163] K. El, K. Isam, J. Raed, Numerical simulation and evaluation of spacer - filled direct contact
1724 membrane distillation module, Appl. Water Sci. 10 (2020) 1–17.
1725 https://doi.org/10.1007/s13201-020-01261-9.

1726 [164] S. Al-Sharif, M. Albeirutty, A. Cipollina, G. Micale, Modelling flow and heat transfer in
1727 spacer-filled membrane distillation channels using open source CFD code, Desalination.
1728 311 (2013) 103–112. https://doi.org/10.1016/j.desal.2012.11.005.

1729 [165] A. Ali, M.M. Agha Shirazi, L. Nthunya, R. Castro-Muñoz, N. Ismail, N. Tavajohi, G.
1730 Zaragoza, C.A. Quist-Jensen, Progress in module design for membrane distillation,

1731 Desalination. 581 (2024) 117584. https://doi.org/10.1016/j.desal.2024.117584.

1732 [166] A. Ali, P. Aimar, E. Drioli, Effect of module design and flow patterns on performance of
1733 membrane distillation process, Chem. Eng. J. 277 (2015) 368–377.
1734 https://doi.org/10.1016/j.cej.2015.04.108.

1735 [167] M.M. Teoh, S. Bonyadi, T.S. Chung, Investigation of different hollow fiber module designs
1736 for flux enhancement in the membrane distillation process, J. Memb. Sci. 311 (2008) 371–
1737 379. https://doi.org/10.1016/j.memsci.2007.12.054.

1738 [168] L. Gao, J. Zhang, S. Gray, J. De Li, Influence of PGMD module design on the water
1739 productivity and energy efficiency in desalination, Desalination. 452 (2019) 29–39.
1740 https://doi.org/10.1016/j.desal.2018.10.005.

1741 [169] V.T. Shahu, S.B. Thombre, Air gap membrane distillation: A review, J. Renew. Sustain.
1742 Energy. 11 (2019). https://doi.org/10.1063/1.5063766.

1743 [170] B.G. Im, L. Francis, R. Santosh, W.S. Kim, N. Ghaffour, Y.D. Kim, Comprehensive insights
1744 into performance of water gap and air gap membrane distillation modules using hollow fiber
1745 membranes, Desalination. 525 (2022) 1–15. https://doi.org/10.1016/j.desal.2021.115497.

1746 [171] R. Tian, H. Gao, X.H. Yang, S.Y. Yan, S. Li, A new enhancement technique on air gap
1747 membrane distillation, Desalination. 332 (2014) 52–59.
1748 https://doi.org/10.1016/j.desal.2013.10.016.

1749 [172] A.E. Khalifa, Flux enhanced water gap membrane distillation process-circulation of gap
1750 water, Sep. Purif. Technol. 231 (2020) 1–9. https://doi.org/10.1016/j.seppur.2019.115938.

1751 [173] X. Yang, R. Wang, A.G. Fane, C.Y. Tang, I.G. Wenten, Membrane module design and
1752 dynamic shear-induced techniques to enhance liquid separation by hollow fiber modules:
1753 A review, Desalin. Water Treat. 51 (2013) 3604–3627.

https://doi.org/10.1080/19443994.2012.751146.

[174] D. Winter, J. Koschikowski, F. Gross, D. Maucher, D. Düver, M. Jositz, T. Mann, A. Hagedorn, Comparative analysis of full-scale membrane distillation contactors - methods and modules, J. Memb. Sci. 524 (2017) 758–771. https://doi.org/10.1016/j.memsci.2016.11.080.

[175] D. Winter, J. Koschikowski, M. Wieghaus, Desalination using membrane distillation: Experimental studies on full scale spiral wound modules, J. Memb. Sci. 375 (2011) 104–112. https://doi.org/10.1016/j.memsci.2011.03.030.

[176] R. Ullah, M. Khraisheh, R.J. Esteves, J.T. McLeskey, M. AlGhouti, M. Gad-el-Hak, H. Vahedi Tafreshi, Energy efficiency of direct contact membrane distillation, Desalination. 433 (2018) 56–67. https://doi.org/10.1016/j.desal.2018.01.025.

[177] L. Eykens, I. Hitsov, K. De Sitter, C. Dotremont, L. Pinoy, I. Nopens, B. Van der Bruggen, Influence of membrane thickness and process conditions on direct contact membrane distillation at different salinities, J. Memb. Sci. 498 (2016) 353–364. https://doi.org/10.1016/j.memsci.2015.07.037.

[178] M. Afsari, M.M.A. Shirazi, A.H. Ghorbani, O. Sayar, H.K. Shon, L.D. Tijing, Triple-layer nanofiber membrane with improved energy efficiency for treatment of hypersaline solution via membrane distillation, J. Environ. Chem. Eng. 11 (2023) 110638. https://doi.org/10.1016/j.jece.2023.110638.

[179] R. Baghel, S. Kalla, S. Upadhyaya, S.P. Chaurasia, K. Singh, CFD modeling of vacuum membrane distillation for removal of Naphthol blue black dye from aqueous solution using COMSOL multiphysics, Chem. Eng. Res. Des. 158 (2020) 77–88. https://doi.org/10.1016/j.cherd.2020.03.016.

[180] B. Lian, Y. Wang, P. Le-Clech, V. Chen, G. Leslie, A numerical approach to module design for crossflow vacuum membrane distillation systems, J. Memb. Sci. 510 (2016) 489–496. https://doi.org/10.1016/j.memsci.2016.03.041.

[181] B. Haddadi, C. Jordan, M. Miltner, M. Harasek, Membrane modeling using CFD: Combined evaluation of mass transfer and geometrical influences in 1D and 3D, J. Memb. Sci. 563 (2018) 199–209. https://doi.org/10.1016/j.memsci.2018.05.040.

[182] Q. Ma, L. Tong, C. Wang, G. Cao, H. Lu, J. Li, X. Liu, X. Feng, Z. Wu, Simulation and Experimental Investigation of the Vacuum-Enhanced Direct Membrane Distillation Driven by a Low-Grade Heat Source, Membranes (Basel). 12 (2022). https://doi.org/10.3390/membranes12090842.

[183] A. Yadav, R.V. Patel, C.P. Singh, P.K. Labhasetwar, V.K. Shahi, Experimental study and numerical optimization for removal of methyl orange using polytetrafluoroethylene membranes in vacuum membrane distillation process, Colloids Surfaces A Physicochem. Eng. Asp. 635 (2022) 1–14. https://doi.org/10.1016/j.colsurfa.2021.128070.

[184] F. Banat, S. Al-Asheh, M. Qtaishat, Treatment of waters colored with methylene blue dye by vacuum membrane distillation, Desalination. 174 (2005) 87–96. https://doi.org/10.1016/j.desal.2004.09.004.

[185] M. Hu, B. Mi, Layer-by-layer assembly of graphene oxide membranes via electrostatic interaction, J. Memb. Sci. 469 (2014) 80–87. https://doi.org/10.1016/j.memsci.2014.06.036.

[186] N.C. Homem, N. de Camargo Lima Beluci, S. Amorim, R. Reis, A.M.S. Vieira, M.F. Vieira, R. Bergamasco, M.T.P. Amorim, Surface modification of a polyethersulfone microfiltration membrane with graphene oxide for reactive dyes removal, Appl. Surf. Sci. 486 (2019) 499–

507. https://doi.org/10.1016/j.apsusc.2019.04.276.

[187] T.J. Mpala, H. Richards, A. Etale, O.T. Mahlangu, L.N. Nthunya, Carbon nanotubes and silver nanoparticles modification of PVDF membranes for improved seawater desalination in direct contact membrane distillation, Front. Membr. Sci. Technol. 2 (2023) 1–11. https://doi.org/10.3389/frmst.2023.1165678.

[188] S.S. Ray, H.S. Bakshi, R. Dangayach, R. Singh, C.K. Deb, M. Ganesapillai, S.S. Chen, M.K. Purkait, Recent developments in nanomaterials-modified membranes for improved membrane distillation performance, Membranes (Basel). 10 (2020) 1–29. https://doi.org/10.3390/membranes10070140.

[189] D.I. Petukhov, D.J. Johnson, Membrane modification with carbon nanomaterials for fouling mitigation: a review, Adv. Colloid Interface Sci. 327 (2024) 103140. https://doi.org/10.1016/j.cis.2024.103140.

[190] I. Tournis, D. Tsiourvas, Z. Sideratou, L.G. Boutsika, A. Papavasiliou, N.K. Boukos, A.A. Sapalidis, Superhydrophobic nanoparticle-coated PVDF-HFP membranes with enhanced flux, anti-fouling and anti-wetting performance for direct contact membrane distillation-based desalination, Environ. Sci. Water Res. Technol. 8 (2022) 2373–2380. https://doi.org/10.1039/d2ew00407k.

[191] M. Huang, J. Song, Q. Deng, T. Mu, J. Li, Novel electrospun ZIF/PcH nanofibrous membranes for enhanced performance of membrane distillation for salty and dyeing wastewater treatment, Desalination. 527 (2022) 115563. https://doi.org/10.1016/j.desal.2022.115563.

[192] Y. Yun, R. Ma, W. Zhang, A.G. Fane, J. Li, Direct contact membrane distillation mechanism for high concentration NaCl solutions, Desalination. 188 (2006) 251–262.

https://doi.org/10.1016/j.desal.2005.04.123.

[193] K.G. Pavithra, S.K. P., V. Jaikumar, S.R. P., Removal of colorants from wastewater: A review on sources and treatment strategies, J. Ind. Eng. Chem. 75 (2019) 1–19. https://doi.org/10.1016/j.jiec.2019.02.011.

[194] V. Calabro, E. Drioli, F. Matera, Membrane distillation in the textile wastewater treatment, Desalination. 83 (1991) 209–224. https://doi.org//10.1016/0011-9164(91)85096-D.

[195] P.J. Lin, M.C. Yang, Y.L. Li, J.H. Chen, Prevention of surfactant wetting with agarose hydrogel layer for direct contact membrane distillation used in dyeing wastewater treatment, J. Memb. Sci. 475 (2015) 511–520. https://doi.org/10.1016/j.memsci.2014.11.001.

[196] Z. Yan, X. Chen, S. Bao, H. Chang, H. Liu, G. Fan, Q. Wang, X. Fu, F. Qu, H. Liang, Integration of in situ Fenton-like self-cleaning and photothermal membrane distillation for wastewater treatment via Co-MoS2/CNT catalytic membrane, Sep. Purif. Technol. 303 (2022) 122207. https://doi.org/10.1016/j.seppur.2022.122207.

[197] W.J. Musnicki, N.W. Lloyd, R.J. Phillips, S.R. Dungan, Diffusion of sodium dodecyl sulfate micelles in agarose gels, J. Colloid Interface Sci. 356 (2011) 165–175. https://doi.org/10.1016/j.jcis.2010.12.067.

[198] P.E. Ohale, C.E. Onu, J.T. Nwabanne, C.O. Aniagor, C.F. Okey-Onyesolu, N.J. Ohale, A comparative optimization and modeling of ammonia–nitrogen adsorption from abattoir wastewater using a novel iron-functionalized crab shell, Appl. Water Sci. 12 (2022) 1–27. https://doi.org/10.1007/s13201-022-01713-4.

[199] R. de S. Silva, H. Ramlow, C.D.Á.K. Cavalcanti, R. de C.S.C. Valle, R.A.F. Machado, C. Marangoni, Steady state evaluation with different operating times in the direct contact

membrane distillation process applied to water recovery from dyeing wastewater, Sep. Purif. Technol. 230 (2020) 2–10. https://doi.org/10.1016/j.seppur.2019.115892.

[200] V.E. Sathishkumar, A.G. Ramu, J. Cho, Machine learning algorithms to predict the catalytic reduction performance of eco-toxic nitrophenols and azo dyes contaminants (Invited Article), Alexandria Eng. J. 72 (2023) 673–693. https://doi.org/10.1016/j.aej.2023.04.007.

[201] M. Fan, J. Hu, R. Cao, W. Ruan, X. Wei, A review on experimental design for pollutants removal in water treatment with the aid of artificial intelligence, Chemosphere. 200 (2018) 330–343. https://doi.org/10.1016/j.chemosphere.2018.02.111.

[202] K. Aghilesh, A. Kumar, S. Agarwal, M.C. Garg, H. Joshi, Use of artificial intelligence for optimizing biosorption of textile wastewater using agricultural waste, Environ. Technol. (United Kingdom). 44 (2023) 22–34. https://doi.org/10.1080/09593330.2021.1961874.

[203] A. Holzinger, K. Keiblinger, P. Holub, K. Zatloukal, H. Müller, AI for life: Trends in artificial intelligence for biotechnology, N. Biotechnol. 74 (2023) 16–24. https://doi.org/10.1016/j.nbt.2023.02.001.

[204] A. Krogh, What are artificial neural networks?, Nat. Biotechnol. 26 (2008) 195–197. https://doi.org/10.1038/nbt1386.

[205] A.H. Sadek, M.K. Mostafa, Preparation of nano zero-valent aluminum for one-step removal of methylene blue from aqueous solutions: cost analysis for scaling-up and artificial intelligence, Appl. Water Sci. 13 (2023) 1–23. https://doi.org/10.1007/s13201-022-01837-7.

[206] M.M. Elshfai, R.G. Hassan, A.S. Mahmoud, Reduction of Biological Contaminants from Municipal Wastewater by Encapsulated nZVI in Alginate (Ag) Polymer: Reduction Mechanism with Artificial Intelligence Approach, Key Eng. Mater. 921 (2022) 173–189.

https://doi.org/10.4028/p-pk7pa4.

[207] A.S. Mahmoud, M.K. Mostafa, M. Nasr, Regression model, artificial intelligence, and cost estimation for phosphate adsorption using encapsulated nanoscale zero-valent iron, Sep. Sci. Technol. 54 (2019) 13–26. https://doi.org/10.1080/01496395.2018.1504799.

[208] R. Ahmad Aftab, S. Zaidi, A. Aslam Parwaz Khan, M. Arish Usman, A.Y. Khan, M. Tariq Saeed Chani, A.M. Asiri, Removal of congo red from water by adsorption onto activated carbon derived from waste black cardamom peels and machine learning modeling, Alexandria Eng. J. 71 (2023) 355–369. https://doi.org/10.1016/j.aej.2023.03.055.

[209] W.S. Noble, What is a support vector machine?, Nat. Biotechnol. 24 (2006) 1565–1567. https://doi.org/10.1038/nbt1206-1565.

[210] Y. Subramanian, J. Gajendiran, R. Veena, A.K. Azad, V.C.B. Sabarish, S.A. Muhammed Ali, A. Kumar, R.K. Gubendiran, Structural, Photoabsorption and Photocatalytic Characteristics of BiFeO3-WO3 Nanocomposites: An Attempt to Validate the Experimental Data Through SVM-Based Artificial Intelligence (AI), J. Electron. Mater. 52 (2023) 2421–2431. https://doi.org/10.1007/s11664-022-10188-7.

[211] F. Hosseini, M. Rahimi, Experimental Study and Artificial Intelligence Modeling of Dye Removal in Microfluidic Systems, Chem. Eng. Technol. 46 (2023) 987–996. https://doi.org/10.1002/ceat.202300105.

[212] Z.H. Jaffari, A. Abbas, S.M. Lam, S. Park, K. Chon, E.S. Kim, K.H. Cho, Machine learning approaches to predict the photocatalytic performance of bismuth ferrite-based materials in the removal of malachite green, J. Hazard. Mater. 442 (2023) 130031. https://doi.org/10.1016/j.jhazmat.2022.130031.

[213] C.A. Buckner, R.M. Lafrenie, J.A. Dénommée, J.M. Caswell, D.A. Want, G.G. Gan, Y.C.

Leong, P.C. Bee, E. Chin, A.K.H. Teh, S. Picco, L. Villegas, F. Tonelli, M. Merlo, J. Rigau, D. Diaz, M. Masuelli, S. Korrapati, P. Kurra, S. Puttugunta, S. Picco, L. Villegas, F. Tonelli, M. Merlo, J. Rigau, D. Diaz, M. Masuelli, M. Tascilar, F.A. de Jong, J. Verweij, R.H.J. Mathijssen, Membrane Distillation: Basics, Advances, and Applications, in: Adv. Membr. Technol., INTECH, 2016: pp. 1–21. https://www.intechopen.com/books/advanced-biometric-technologies/liveness-detection-in-biometrics.

[214] N.M. Mokhtar, W.J. Lau, A.F. Ismail, The potential of membrane distillation in recovering water from hot dyeing solution, J. Water Process Eng. 2 (2014) 71–78. https://doi.org/10.1016/j.jwpe.2014.05.006.

[215] P.S. Goh, K.C. Wong, A.F. Ismail, Membrane technology: A versatile tool for saline wastewater treatment and resource recovery, Desalination. 521 (2022) 115377. https://doi.org/10.1016/j.desal.2021.115377.

[216] R. Castro-Munoz, K. V Agrawal, Z. Lai, J. Coronas, Towards large-scale application of nanoporous materials in membranes for separation of energy-relevant gas mixtures, Sep. Purif. Technol. 308 (2023) 122919. https://doi.org/10.1016/j.seppur.2022.122919.

[217] C.M. Tolentino Filho, R. de S. Silva, C.D.Á.K. Cavalcanti, M.A. Granato, R.A.F. Machado, C. Marangoni, Membrane distillation for the recovery textile wastewater: Influence of dye concentration, J. Water Process Eng. 46 (2022) 102611. https://doi.org/10.1016/j.jwpe.2022.102611.

[218] L.N. Nthunya, L. Gutierrez, N. Khumalo, S. Derese, B.B. Mamba, A.R. Verliefde, S.D. Mhlanga, Superhydrophobic PVDF nanofibre membranes coated with an organic fouling resistant hydrophilic active layer for direct-contact membrane distillation, Colloids Surfaces A Physicochem. Eng. Asp. 575 (2019) 363–372. https://doi.org/10.1016/j.colsurfa.2019.05.031.

[219] H.B. Madalosso, R. de Sousa Silva, A. Merlini, R. Battisti, R.A.F. Machado, C. Marangoni, Modeling and experimental validation of direct contact membrane distillation applied to synthetic dye solutions, J. Chem. Technol. Biotechnol. 96 (2021) 909–922. https://doi.org/10.1002/jctb.6599.

[220] A.S. Alsaadi, N. Ghaffour, J.D. Li, S. Gray, L. Francis, H. Maab, G.L. Amy, Modeling of air-gap membrane distillation process: A theoretical and experimental study, J. Memb. Sci. 445 (2013) 53–65. https://doi.org/10.1016/j.memsci.2013.05.049.

[221] W. Li, Y. Chen, L. Yao, X. Ren, Y. Li, L. Deng, Fe3O4/PVDF-HFP photothermal membrane with in-situ heating for sustainable, stable and efficient pilot-scale solar-driven membrane distillation, Desalination. 478 (2020) 114288. https://doi.org/10.1016/j.desal.2019.114288.

[222] A. Politano, P. Argurio, G. Di Profio, V. Sanna, A. Cupolillo, S. Chakraborty, H.A. Arafat, E. Curcio, Photothermal Membrane Distillation for Seawater Desalination, Adv. Mater. 29 (2017) 1–6. https://doi.org/10.1002/adma.201603504.

[223] A.G. Razaqpur, Y. Wang, X. Liao, Y. Liao, R. Wang, Progress of photothermal membrane distillation for decentralized desalination: A review, Water Res. 201 (2021) 117299. https://doi.org/10.1016/j.watres.2021.117299.

[224] Y.S. Jun, X. Wu, D. Ghim, Q. Jiang, S. Cao, S. Singamaneni, Photothermal Membrane Water Treatment for Two Worlds, Acc. Chem. Res. 52 (2019) 1215–1225. https://doi.org/10.1021/acs.accounts.9b00012.

[225] L. Zhang, C. Sha, B. Li, W. Wang, Investigation of utilizing carbonized lotus root as photothermal material in the solar steam generation system, Energy Sources, Part A Recover. Util. Environ. Eff. 45 (2023) 3359–3368. https://doi.org/10.1080/15567036.2023.2196953.

1939

1940

Highlights

- Discharge of dye effluent requires robust and cost-effective treatment processes
- Membrane distillation emerged as a promising tool towards dye remediation
- The current study reviewed research advancement towards environmental dye remediation
- However, fouling and thermal efficiency of MD remain a major challenge
- The reviewed study suggested optimization of membrane and module designs for effective dye remediation

Declaration of interests

The authors declare that they have no known competing financial interests or personal relationships that could have appeared to influence the work reported in this paper.